



저작자표시-비영리-변경금지 2.0 대한민국

이용자는 아래의 조건을 따르는 경우에 한하여 자유롭게

- 이 저작물을 복제, 배포, 전송, 전시, 공연 및 방송할 수 있습니다.

다음과 같은 조건을 따라야 합니다:



저작자표시. 귀하는 원저작자를 표시하여야 합니다.



비영리. 귀하는 이 저작물을 영리 목적으로 이용할 수 없습니다.



변경금지. 귀하는 이 저작물을 개작, 변형 또는 가공할 수 없습니다.

- 귀하는, 이 저작물의 재이용이나 배포의 경우, 이 저작물에 적용된 이용허락조건을 명확하게 나타내어야 합니다.
- 저작권자로부터 별도의 허가를 받으면 이러한 조건들은 적용되지 않습니다.

저작권법에 따른 이용자의 권리는 위의 내용에 의하여 영향을 받지 않습니다.

이것은 [이용허락규약\(Legal Code\)](#)을 이해하기 쉽게 요약한 것입니다.

[Disclaimer](#)

2018 年 8 月
博士學位論文

Coumestrol-induced apoptosis and
its cellular signaling pathways in
FaDu human hypopharynx squamous
carcinoma

朝鮮大學校 大學院

齒醫生命工學科

趙 仁 我

Coumestrol에 의한 FaDu 인후두암세포 사멸 및 세포 생체 신호전달기전

Coumestrol-induced apoptosis and its cellular
signaling pathways in FaDu human hypopharynx
squamous carcinoma

2018年 8月 24日

朝鮮大學校 大學院

齒醫生命工學科

趙 仁 我

Coumestrol-induced apoptosis and its cellular signaling pathways in FaDu human hypopharynx squamous carcinoma

指導教授 金 秀 官

이 論文을 理學 博士學位신청 論文으로 提出함.


2018 年 4 月

朝鮮大學校 大學院

齒醫生命工學科


趙 仁 我


趙仁娥의 碩士學位論文을 認准함

委員長 朝鮮大學校 教授 김춘성 

委員 서울大學校 教授 김영균 

委員 朝鮮大學校 教授 이숙영 

委員 朝鮮大學校 教授 김재성 

委員 朝鮮大學校 教授 김수관 

2018 年 6 月

朝鮮大學校 大學院

CONTENTS

CONTENTS	i
List of Figures	iv
List of Abbreviations	vii
국문초록	ix
I. Introduction	1
II. Materials and Methods	6
II- 1. Chemicals and antibodies	6
II- 2. Cell line and cell culture	6
II- 3. Cell viability by MTT assay	7
II- 4. Cell live & dead assay	7
II- 5. Hematoxylin & eosin staining	8
II- 6. Nuclear staining using DAPI	8
II- 7. DNA fragmentation assay	9
II- 8. Cell apoptosis analysis by flow cytometry	9
II- 9. Western blot analysis	10
II-10. Caspase-3/-7 activity assay	11
II-11. Caspase dependent cell survival assay	11
II-12. Colony formation assay	12
II-13. Migration assay	12
II-14. Invasion assay	13
II-15. Gelatin zymography	13
II-16. Xenograft mouse model	14
II-17. Histology and immunohistochemistry	14
II-18. Statistical analysis	15

III. Results	16
III- 1. Coumestrol exerts dose-dependent cytotoxicity in FaDu cells, but not in L929.	16
III- 2. Coumestrol reduces the survival of FaDu cells, but did not affect L929.	19
III- 3. Formation of apoptotic bodies increases in FaDu cells treated with coumestrol.	22
III- 4. Coumestrol elevates the number of FaDu cells with chromatin-condensed nuclei.	24
III- 5. Coumestrol induces the DNA fragmentation in FaDu cells.	26
III- 6. Coumestrol increases the proportion of apoptotic FaDu cells.	28
III- 7. Coumestrol-induced FaDu cell death is mediated by apoptosis through the death receptor-mediated (extrinsic) and mitochondria-dependent (intrinsic) pathways.	30
III- 8. Coumestrol-induced FaDu cell apoptosis is dependent on the activation of caspase-3.	35
III- 9. Coumestrol suppresses colony formation in FaDu cells.	40
III-10. Coumestrol attenuates effectively the migration of FaDu cell.	42
III-11. Coumestrol suppresses the invasion of FaDu cells.	44
III-12. Downstream molecules affect the metastatic suppression of coumestrol in FaDu cells.	46
III-13. Coumestrol-induced antitumor effects are mediated by alterations in the PI3K/Akt-mTOR axis and MAPK cellular signaling pathways in FaDu cells.	48
III-14. Antitumor effects of coumestrol in the animals xenografted with FaDu cells.	53

IV. Discussion 56

V. Reference 68

감사의 글 75

List of Figures

Figure 1. Chemical structure of coumestrol.	5
Figure 2. Coumestrol does not affect the viability of L929, used as the normal cells.	17
Figure 3. Coumestrol increases the cytotoxicity in FaDu cells.	18
Figure 4. Coumestrol does not affect the survival of L929, used as the normal cells.	20
Figure 5. Coumestrol reduces the survival of FaDu cells.	21
Figure 6. Coumestrol increases the formation of apoptotic bodies formation in FaDu cells.	23
Figure 7. Coumestrol increases the number of FaDu cells with chromatin-condensed nuclei.	25
Figure 8. DNA fragmentation dose-dependently increases in FaDu cells treated with coumestrol.	27
Figure 9. Coumestrol dose-dependently increases the proportion of FaDu cells undergoing apoptosis.	29
Figure 10. Cleaved caspase-8, a death receptor-mediated (extrinsic) pro-apoptotic factor, is dose-dependently increased by the expression of FasL in FaDu cells treated with coumestrol.	31

Figure 11. Mitochondrial-dependent intrinsic apoptosis is involved with FaDu cell death mediated by coumestrol. 32

Figure 12. Coumestrol induces FaDu cell death through the activation of caspase-3 and poly(ADP ribose)polymerase (PARP). 33

Figure 13. The activity of caspase-3/-7 is dose-dependently upregulated in FaDu cells treated with coumestrol. 35

Figure 14. Coumestrol-induced FaDu cell apoptosis is dependent on caspase activation. 37

Figure 15. Pan-caspase inhibitor, Z-VAD-FMK suppresses apoptotic cell death in FaDu cells treated with coumestrol. 38

Figure 16. Coumestrol suppresses the colony formation through the attenuation of FaDu cell proliferation. 41

Figure 17. Migration decreases in FaDu cells treated with coumestrol. 43

Figure 18. Coumestrol suppresses the invasion of FaDu cells. 45

Figure 19. The expression and activity of MMP-2 and MMP-9 decreases in FaDu cells treated with coumestrol. 47

Figure 20. Coumestrol suppresses the phosphorylation of Akt and its downstream factor mTOR, but increases the tumor suppressor p53 in FaDu cells. 49

Figure 21. Coumestrol increases the cell-cycle arrest markers p21 and p27 in FaDu cells. 50

Figure 22. Coumestrol-induced cell anti-proliferation and apoptosis is mediated by the suppression of MAPK in FaDu cells. 51

Figure 23. Coumestrol inhibits the growth of FaDu tumors in a xenograft animal model. 54

Figure 24. Coumestrol-induced antitumor effects are mediated by the modulation of the Akt cellular signaling pathway and upregulation of tumor suppressor p53 in the FaDu xenograft animal model. 55

Figure 25. Schematic diagram of the coumestrol-induced apoptotic phenomenon. 65

Figure 26. Schematic diagram of coumestrol-induced apoptosis pathways. 66

Figure 27. Schematic diagram of cellular signaling pathways associated with the coumestrol-induced inhibition of migration and invasion in FaDu cells. 67

List of Abbreviations

American Type Culture Collection	ATCC
Bcl-2-associated death promoter	Bad
BCL2-antagonist/killer 1	Bak
Bcl-2-associated X protein	Bax
bicinchoninic acid protein assay	BCA
B-cell lymphoma 2	Bcl-2
B-cell lymphoma extra-large	Bcl-XI
Bax-like BH3 protein	Bid
Cyclin-dependent kinases	CDK
4' 6' -diamidino-2-phenyl indole dihydro chloride	DAPI
Dulbecco's modified Eagle's medium	DMEM
dimethyl sulfoxide	DMSO
Dulbecco's phosphate-buffered saline	DPBS
extracellular signal-regulated kinases	ERK1/2
Fas-associated protein with death domain	FADD
fetal bovine serum	FBS
Z-Val-Ala-Asp fluoromethyl ketone	Z-VAD-FMK
Hematoxylin & eosin	H&E
Mouse normal connective tissue	L929
Head and neck squamous cell carcinoma	HNSCC
Institutional Animal Care and Use Committee	IACUC
Korea cell line bank	KCLB

Mitogen-activated protein kinase	MAPK
minimum essential medium	MEM
matrix metalloprotease	MMP
mammalian target of rapamycin	mTOR
3-(4, 5-dimethyl thiazol-2-yl)-2, 5-diphenyl tetrazolium bromide	MTT
polyacrylamide gel electrophoresis	PAGE
poly (ADP ribose) polymerase	PARP
phosphate buffered saline	PBS
phosphatidylinositol 3-kinase	PI3K
phosphatidylinositol 4,5-biphosphate	PIP ₂
phosphatidylinositol 3,4,5-triphosphate	PIP ₃
Phosphatase and tensin homolog	PTEN
Standard deviation	SD
sodium dodecyl sulfate	SDS
Tumor necrosis factor	TNF
Tumor necrosis factor receptor type 1-associated domain protein	TRADD
TNF-related apoptosis-inducing ligand	TRAIL

국문초록

Coumestrol에 의한 FaDu 인후두암세포 사멸 및 세포 생체 신호전달기전

조 인 아

지도교수 : 김수관

조선대학교 치의생명공학과 박사과정

인후두암은 일반적으로 구강의 점막 내층에서 발생하며, 대부분 조기 발견이 어렵고 치유율이 낮은 반면 사망률이 매우 높은 암으로 알려져 있다. 현재 임상에서 사용되는 항암 화학 요법제(Chemotherapeutic reagent)는 메스꺼움, 구토, 구내염, 설사 및 골수 기능 장애와 같은 다양한 부작용을 동반함에 따라 부작용이 적으며 암 특이적 세포사멸 유도가 가능한 효과적인 항암 화학 요법제 개발이 절실히 요구되어진다. 최근 부작용이 적은 항암 화학 요법제 개발과 관련하여 생물학적 안전성과 다양한 약리학적 효과를 나타내는 자연에서 유래된 유사체 에스트로젠(Phytoestrogen)에 대한 관심이 높아지고 있는 추세이다. 유사체 에스트로젠은 항산화 및 항염증 등 다양한 생리학적 효능에 대한연구가 보고되고 있을 뿐만 아니라 다양한 암에서 효과적인 항암활성이 보고되고 있다.

Coumestrol은 coumestans 계열의 천연 유기 화합물로 클로버, 시금치, 브루셀스프라우트(Brussels sprouts) 및 콩 등 다양한 식용 가능 식물에 포함된 기능성 물질로 알려져 있다. 최근 coumestrol은 유방암, 전립선 암 및 폐암과 같은 다양한 종류의 암에서 항암 효과가 보고되었지만, 암 세포 사멸 및 전이 억제와 같은 항암 효과는 인후두암에서 아직 조사되지 않았다. 따라서, 본 연구의 목적은 coumestrol의 생물학적 안전성을 분석하고, 이를 토대로 FaDu 인후두암세포에서 항암효능 및 이와 관련된 기전을 분석하여, 최종적으로 생체 내 인후두암에 대한 항암효능을 분석하고자 한다.

Coumestrol의 세포독성을 평가하기 위하여 FaDu 인후두암세포를 10% (w/v)

Fetal Bovine Serum (FBS, Life Technologies, Grand Island, USA)이 포함된 Minimum Essential Medium (MEM, Life Technologies, GRAND Island, NY, USA)배지를 이용하여 5%의 CO₂가 유지되는 37°C CO₂ 배양기에서 24 시간 배양하여 사용하였다. Coumestrol로 처리하여 MTT assay 및 Cell live & dead assay를 수행하여 각각 세포 독성 및 세포생존율을 분석하였다. Hematoxylin & Eosin 염색법, DAPI 염색법, DNA 단편화(DNA fragmentation) 분석을 사용하여 각각 아포토시스소체(apoptotic body) 형성, 핵 응축 및 DNA 분절현상 등 아포토시스(Apoptosis)와 관련된 세포사멸 현상을 분석하였다. 또한, 유세포 분석(Fluorescence activated cell sorter)을 이용하여 coumestrol에 의한 FaDu 인후두암세포의 아포토시스를 검증하였다. Western blot과 caspase-3 /-7 activity assay를 이용하여 아포토시스 및 이와 관련된 세포 신호 전달 경로를 분석하였다. 콜로니 형성(colony formation), 트랜스 웰 분석 및 상처 치유(wound healing)분석을 수행하여 각각 증식(proliferation), 침입(invasion) 및 이동(migration)을 분석하였다. 최종적으로, FaDu 인후두암세포 이식을 통하여 제작된 동물모델을 활용하여 coumestrol에 대한 생체 대상 항종양 효과 및 이에 대한 기전을 면역조직화학법(immunohistochemistry)을 수행하여 분석하였다.

Coumestrol은 FaDu 인후두암세포 사멸을 유의하게 증가 시켰으며, 정상 사람 구강 각화 세포(human normal oral keratinocyte)의 생존력에는 영향을 미치지 않았다. Coumestrol으로 48시간 동안 FaDu 인후두암세포를 처리 할 때 형태학적 변화와 핵응축, DNA 분절화, 세포 사멸 개체군의 증가와 같은 아포토시스의 전형적인 특성이 증가했다. 또한, coumestrol은 FaDu 인후두암세포에서 세포사멸유도인자인 FasL의 발현을 용량 의존적으로 유의하게 증가시켜 이의 하위 세포사멸인자인 caspase-8을 활성화를 통한 외인성세포사멸경로(death receptor-mediated apoptosis) 매개됨을 확인하였다. 뿐만 아니라 활성화된 caspase-8에 의하여 세포사멸인자인 Bid를 tBid로 활성화하여 Bax 및 Bad 등의 발현증가 및 세포사멸억제인자인 Bcl-2 및 Bcl-xL의 발현을 감소시킴으로써 미토콘드리아 막 전위(mitochondria membrane potential)을 감소시켜 cytochrom c를 세포질로 분비시킴으로써 caspase-9 활성화를 통한 미토콘드리아 의존 내인성 세포사멸(mitochondria dependent intrinsic apoptosis)에 의한 FaDu 인후두암세포 사멸이 매개됨을 확인하였다. 최종적으로 활성화된 각각의 외인성 및 내인성 세포사멸인

자인 caspase-8 및 caspase-9에 의한 단계적인 caspase-3 및 poly ADP ribose polymerase (PARP)의 활성화가 매개됨을 확인하였다. 또한, caspase inhibitor인 Z-VAD-FMK를 이용하여 caspase 활성억제에 따른 coumestrol의 caspase 의존적인 세포사멸현상임을 확인하였다. 특히, 본 연구에서는 coumestrol에 의해 유발된 FaDu 인후두암세포 사멸은 ERK1/2 및 p38을 포함하는 mitogen-activated protein kinase (MAPK)의 인산화를 억제시킬 뿐만 아니라 Akt-mTOR 세포신호 전달경로를 통한 p-53 발현 상향 조절에 의해 매개되었다. 또한, 본 연구에서는 암세포 증식 및 이동과 관련된 중요한 인자인 matrix metalloproteinase (MMP)-2 및 MMP-9 발현과 활성이 coumestrol 농도의존적으로 억제됨으로써 FaDu 인후두암 세포의 증식, 이동 및 침입이 억제 또는 지연되는 coumestrol의 암세포 전이 억제 효능을 확인하였다. 최종적으로 coumestrol에 의한 세포사멸, 암세포 증식 및 전이 억제효능에 대한 생체 내 효능을 분석한 결과 FaDu 인후두암세포가 이식된 종양동물모델에서 유의하게 종양형성이 억제됨을 확인하였다. 종양동물로부터 회수된 종양조직에 대한 면역조직화학적 분석을 시행한 결과 coumestrol 경구 투여된 종양 내 Akt의 인산화가 억제되어있는 반면, 대표적인 종양억제인자인 p53의 발현이 유의적으로 증가되어있음을 확인하였다.

이러한 연구결과를 토대로 coumestrol은 FaDu 인후두암종에서 내인성 및 외인성세포사멸경로를 통한 세포사멸을 유도할 뿐만 아니라 Akt-mTOR 및 MAPK 신호전달경로를 통하여 종양억제인자인 p53의 발현증가를 통하여 암세포의 증식 및 전이를 억제시키는 다양한 항종양효능이 *in vitro* 및 *in vivo* 연구에서 확인되었다. 따라서, 이러한 결과는 coumestrol 두경부 인후두암종 치료를 위한 생물학적 안전성 및 우수한 항암효과가 확보된 화학 치료제 후보물질임을 제시하고 있다.

I . Introduction

Head and neck squamous cell carcinoma (HNSCC) generally develops in the mucosal lining of the oral cavity, pharynx, larynx, salivary glands, paranasal sinuses and nasal cavity (Jemal et al., 2007). More than approximately 640,000 new cases of HNSCC are reported annually and account for 4% of all cancer-related deaths globally (Chen and Hu, 2010). HNSCC is reported as the sixth most common cancer and has a high mortality rate (Guenin et al., 2014).

The general clinical symptoms of HNSCC are known to include unusual ulcers or pain, sore throat, troubled breathing, discomfort when swallowing, swelling under the jawbone or around the salivary glands, and paralysis of the muscles in the face (Jakobi et al., 2015). Although large studies associated with the investigation of the pathophysiological factors of HNSCC are in progress, its specific pathological etiologies remain largely unknown (Galbiatti et al., 2013). However, recent studies have reported that consumption of alcohol, and smokeless tobacco, and chewing tobacco are major risk factors in at least 75% of HNSCC (Hashibe et al., 2009). The risk factors for HNSCC disease include human papillomavirus (HPV) infection are 2 to 6 times higher than the one in the general population (Ceccarelli et al., 2018), industrial exposure to nickel dust or formaldehyde (Luce et al., 1993), Epstein-Barr virus infection (Chien et al., 2001), and Asian ancestry (mainly Chinese descent) (Yu and Yuan, 2002). Furthermore, the explosive global increase in the elderly population will also increase, the prevalence of patients diagnosed with HNSCC (Boscolo-Rizzo et al., 2018). The clinical management of patients with HNSCC encompasses surgical procedures, radiotherapy, chemotherapy, or a combination of in the clinical therapies (Galbiatti et al., 2013). Although surgical procedures are the most frequently performed clinical management strategy for patients with HNSCC, they may result in many side effects, such as the alteration of chewing, or swallowing functions, effects on

speech, and facial deformity of patients after surgery. Although the non-surgical management strategy of radiotherapy has exhibited clinical efficacy, it also is accompanied by many side effects, such as redness, irritation, and inflammation of the mouth (Shrotriya et al., 2015). Furthermore, radiotherapy can result in a dry mouth and dysphagia caused by destruction of the salivary glands; in addition, nutritional imbalances occur caused by the reduction of appetite through the loss of taste (Pinna et al., 2015). Moreover, patients with HNSCC are frequently treated with chemotherapy, either alone or in combination with radiotherapy, after surgical procedures; although chemotherapy is able adequately to induce cancer cell death, it is potentially cytotoxic to healthy cells, and chemotherapy is, therefore, accompanied by many side effects, including nausea, vomiting, stomatitis, diarrhea, and bone marrow dysfunction. Consequently, despite the rapid progression in the field of medicine, the five-year survival rate and mortality of patients diagnosed with HNSCC have not improved significantly over the past 40 years. (Radhakrishnan et al., 2016). Collectively, these factors indicate the requirement for new clinical management strategies, able to effectively induce cancer cell death with fewer side effects, for patients with HNSCC.

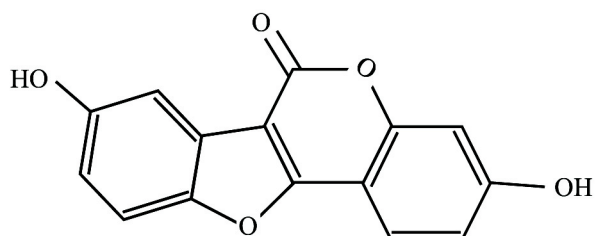
Recent strategies of using chemotherapeutic agents for the management of patients with cancer have targeted cancer-specific cell death through the induction of apoptosis, inhibition of migration and invasion, and cancer cell cycle arrest (Lu et al., 2011). The development of strategies for using chemotherapeutic reagents based on the induction of apoptosis, as known as programmed cell death, has focused on the acceleration of programmed cancer-specific cell death through the activation of apoptotic factors. However, the development of chemotherapeutic reagents based on this strategy cannot induce cancer-specific cell death without damaging normal cells, because the cellular biology of cancer cells is similar to that of normal cells (Ricci and Zong, 2006). In addition, cancer cell metastasis is closely associated with migration and invasion (Luo et al., 2018). The primary methods of cancer

metastasis are direct extension, invasion, or when cancer cells break away from a primary tumor and travel to another part of the body through the lymphatic system or, bloodstream (Gupta and Massague, 2006). Thus, this contributes to the increased mortality of patients as the cancer spreads to other organs in the body. Hence, the inhibition of cancer cell migration and invasion is particularly crucial in the development of chemotherapeutic reagents, as metastatic cancer is usually more difficult to treat than cancer that has not spread. In most cases, the goal of treatment for metastatic cancer is to prolong survival and maintain quality of life (Dattatreya, 2013). Therefore, recent studies associated with the development of chemotherapeutic reagents able to effectively induce cancer cell-specific death with fewer side effects have focused on natural compounds purified from herbal plants that are used in traditional folk or oriental medicines.

Traditional medicines based on herbal plants have played an essential part in healthcare in many cultures for thousands of years. Furthermore, many scientific studies have confirmed that natural metabolites originating from herbal plants may offer advantages over synthetic compounds, such as the possibility to transport to the required intracellular site of action (Li and Vederas, 2011). Herbal plants have tremendous potential to provide novel drugs and, as such, are natural chemicals that may be chemoprotective or anticancer agents (Desai et al., 2008). Moreover, recent studies associated with chemotherapies based on the herbal metabolites have reported their high bioavailability, biological activity, and activity as substrates for the transporter systems that deliver the compounds to their target (Taylor and Jabbarzadeh, 2017). Most recently, substances derived from herbal plants were investigated for their biological safety and a wide range of pharmacological effects in many studies (Kinghorn et al., 2011). Among these substances, phytoestrogens, which are polyphenols similar to human estrogens found in plants or derived from plant precursors, comprise several classes of chemical compounds coumestans, isoflavones, ellagitannins, stilbenes, and lignans (Gaya

et al., 2016). Coumestrol is a natural organic compound in the class of coumestans; it is found in various plants, such as clover, soybeans and brussels sprouts (Bacciottini et al., 2007). Clover is known to have antioxidant, anti-inflammatory and anticancer effects (Khorasani Esmaili et al., 2015). Likewise, soybean is known to have anti-inflammatory (Tang et al., 2017), antioxidant, and anti-pain effects in various diseases; both plants contain notable amounts of phytoestrogens (Pandey and Rizvi, 2009).

As shown in Figure 1, coumestrol is an estrogen compound (3,9-dihydroxy-6-benzofurano [3,2-c] chromenone, chemical abstracts service, CAS number: 479-13-3). Many recent studies have reported that coumestrol has anti-inflammatory and antioxidant properties (Jantaratnotai et al., 2013). Although the anticancer effects of coumestrol in various types of cancers, including breast cancer cells (Zafar et al., 2018), prostate cancer, and lung cancer (Reger et al., 2018), have been reported, the anticancer activities, including the induction of apoptosis and the inhibition of metastasis, have not yet been investigated in HNSCC. Therefore, the aim of the present study was to evaluate the potential of coumestrol to induce apoptosis in HNSCC and identify the signaling pathway responsible for apoptosis.



- Coumestrol
- CAS Number : 479-13-0
- IUPAC NAME : 3,9-Dihydroxy-6-benzofurano[3,2-c]chromenone
- Chemical formulation : $C_{15}H_8O_5$
- Molecular mass : 268.22

Figure 1. Chemical structure of coumestrol.

II. Materials and Methods

II-1. Chemicals and antibodies

Coumestrol was purchased from Santa Cruz Biotechnology, Inc. (Dallas, TX, USA) and was dissolved in ethanol at stock concentration (= 100 mM). Antibodies for Fas ligand (FasL, 48 kDa), cleaved caspase-3 (17 and 19 kDa), cleaved caspase-8 (18 kDa), cleaved caspase-9 (37 kDa), poly (ADP ribose) polymerase (PARP, preform 116 kDa and cleaved form 85 kDa), phospho-Erk1/2 (42 and 44 kDa), total-Erk1/2 (42 and 44 kDa), phospho-p38 (38 kDa), total-p38 (38 kDa), and β -actin (45 kDa) were from Cell signaling Technology Inc. (Denver, MA, USA) B-cell lymphoma 2 (Bcl-2, 26 kDa), B-cell lymphoma extra-large (Bcl-xL, 26 kDa), Bcl-2-associated X protein (Bax, 21 kDa), Bax-like BH3 protein (Bid, 22 and 15 kDa), Bcl-2-associated death promoter (Bad, 23 kDa), phospho-Akt (60 and 56 kDa), total Akt (62 kDa), p53 (53 kDa), p21 (21 kDa), p27 (27 kDa), matrix metalloproteinase (MMP-2, 72 and 63 kDa), MMP-9 (92 kDa), and secondary antibodies were purchased from Santa Cruz Biotechnology Inc. (Dallas, TX, USA) Phospho-mTOR (250 kDa) and total-mTOR (250 kDa) was purchased from Life Technologies, (Carlsbad, CA, USA).

II-2. Cell line and cell culture

FaDu cells, a human pharyngeal squamous carcinoma cell line was obtained from the American Type Culture Collection (ATCC, Manassas, VA, USA) and were grown in maintained in minimum essential medium (MEM, Life Technologies, Grand Island, NY, USA). Mouse normal connective tissue (L929) were purchased from Korea cell line bank (KCLB, Seoul, Republic of

Korea). The L929 were maintained in Dulbecco's modified Eagle's medium (DMEM, Life Technologies, Grand Island, NY, USA) containing 10% fetal bovine serum (FBS, Life Technologies, Grand Island, NY, USA). Media which was supplemented with 10% FBS and 1% antibiotics. The cells were maintained in a humidified and 5% CO₂ controlled incubator at 37°C.

II-3. Cell viability by MTT assay

Cell cytotoxic effect of coumestrol on cells was measured by 3-(4-, 5-Dimethylthiazol-2-yl)-2,5-diphenyl tetrazolium bromide (MTT, Life Technologies, Grand Island, NY, USA) assay. Cells seeded on a 96-well culture plate (2×10^4 cells/well) for overnight. After incubation, the cultured cells were treated with 5, 10, 20, or 50 μ M coumestrol for 24, 48, and 72 h at 37° C to determine its dose-dependent effects. After incubation under the defined conditions, cells were incubated for another 4 h in 20 μ L of 5 mg/mL MTT working solution. The supernatant subsequently removed, and MTT crystals dissolved in 200 μ L/well dimethyl sulfoxide (DMSO). After that, optical density was measured at 570 nm using a spectrometer. The experiments were repeated three times, independently. The mean OD \pm standard deviation (SD) for each group of replicates calculated. The entire procedure repeated three times. The inhibitory rate of cell growth was calculated using the equation: % growth inhibition = $[(1 - \text{OD extract treated})/(\text{OD negative control})] \times 100$

II-4. Cell live & dead assay

Cell live & dead assay (Thermo Fisher Scientific, Rockford, IL, USA), which is composed of green calcein AM to stain the live cells with green fluorescence and ethidium homodimer-1 to stain the dead cells with red

fluorescence, was performed to visualize. Briefly, L929 and FaDu cells were cultured at a density of 2×10^4 cells/mL in an 8-well chamber slide (Electron Microscopy Sciences, Hatfield, PA, USA) and allowed to attach to the well overnight. After incubation, cultured L929 and FaDu cells were treated with 0, 25, and 50 μ M coumestrol for 48 h. After treatment, the cells were washed twice with Dulbecco's phosphate-buffered saline (DPBS) after removing the medium. Stained with green calcein AM and ethidium homodimer-1 (1 μ L/ml) at room temperature in the dark for 30 min. After staining, cells were washed three times with DPBS. After that, cells were imaged using fluorescence microscopy (Eclipse TE2000, Nikon Instruments, Melville, NY, USA).

II -5. Hematoxylin & eosin staining

Hematoxylin & eosin (H&E) staining was performed to observe the morphological changes of cells. FaDu cells were cultured at a density of 5×10^4 cells/mL 24 h and then treated with different concentrations 0, 25, and 50 μ M of coumestrol for 48 h at 37° C. After that, cells were rinsed three times with PBS at 4° C and fixed with 4% paraformaldehyde, for 5 min at 4° C. The cells were observed and imaged by microscopy (Eclipse TE2000, Nikon Instruments, Melville, NY, USA).

II -6. Nuclear staining using DAPI

DAPI staining was performed to detection of cells with a condensed nucleus, which is an apoptotic phenomenon. Briefly, L929 and FaDu cells were cultured at a density of 2×10^4 cells/mL in an 8-well chamber slide (Electron Microscopy Sciences, Hatfield, PA, USA) and allowed to attach to the well overnight. After incubation, cultured L929 and FaDu cells treated

with 0, 25, and 50 μ M coumestrol for 48 h. Thereafter, L929 and FaDu cells were fixed with 4% paraformaldehyde after washing with phosphate buffer solution (PBS) and stained with 1 mg/ml DAPI (Sigma-Aldrich, St. Louis, MO, USA) for 20 min. The nucleus of L929 and FaDu cells were imaged using fluorescence microscopy (Eclipse TE2000, Nikon Instruments, Melville, NY, USA).

II-7. DNA fragmentation assay

FaDu cells were collected after treatment with coumestrol (0, 25, and 50 μ M) and incubation for 48 h, and rinsed in PBS at 4 °C. The cells were then treated with 100 μ L of cell lysate buffer (100 mM NaCl, 300 mM EDTA, 200 mM Tris-HCl, pH 7.5) and 10% sodium dodecyl sulfate (SDS) add to incubated at 65 °C for 10 min, then 5 M sodium acetate add to store at 4 °C for 30 min followed by centrifugation at 12,000 $\times g$ for 15 min. RNase A was added to the supernatant and incubated at 37 °C for 1 h. An equal volume of phenol: chloroform: isoamyl alcohol (PCI, Life Technologies, Grand Island, NY, USA) was added then centrifugation at 12,000 $\times g$ for 15 min at 4 °C. The supernatant was incubated at -80 °C for 30 min, then removed after centrifugation at 12,000 $\times g$ for 15 min at 4 °C. The pellet was allowed to dry naturally and was dissolved in TE buffer (10 mM Tris-HCl, pH 7.6, 0.1 mM EDTA), followed by electrophoresis on 1.5% agarose gel. The imaging system was used for observation and images were captured.

II-8. Cell apoptosis analysis by flow cytometry

Flow cytometric analysis (FACS) was performed to detect apoptosis using co-stained with annexin V-FITC and propidium iodide (PI) (Cell Signaling Technology, Danvers, MA, USA). After 5×10^5 cells/mL of FaDu cells were plated into a 6-well culture plate and then treated with coumestrol for 48 h.

Both floating and attached cells were then collected, washed twice with PBS, and resuspended in 500 μ L of $1\times$ binding buffer (BD Biosciences, San Diego, CA, USA). Annexin V-FITC and PI were added to the cells for 15 min at 37° C in the dark. The population of annexin-V-positive cells and the cell cycle phase were analyzed using a BD Cell Quest®version 3.3 instrument (Becton Dickinson, San Jose, CA, USA) and WinMDI version 2.9 software (The Scripps Research Institute, San Diego, CA, USA).

II-9. Western blot analysis

FaDu cells at a density of 1×10^6 cells/mL were plated on culture dishes and incubated for 24 h in a humidified incubator at 37° C in 5% CO₂. FaDu cells treated with coumestrol for 48 h. Thereafter, FaDu cells were harvested and were lysed using a cell lysis buffer (Cell Signaling Technology, Danvers, MA, USA) containing Protease and Phosphatase Inhibitor Cocktails (Life Technologies, Grand Island, NY, USA) and incubated for 1 h at 4° C. Lysates were centrifuged at $14,000 \times g$ for 10 min at 4° C. The supernatant used as the cytosolic fraction. Total protein concentrations of the cell lysates determined by bicinchoninic acid protein assay (BCA Protein Assay Kit, Thermo Scientific, Rockford, IL, USA). Loading 5 \times buffer (250 mM Tris-HCl, pH 6.8, 10% SDS, 30% (v/v) Glycerol, 5% β -mercaptoethanol, bromophenol Blue) was added to equal amounts of protein, and the mixture boiled at 90° C for 10 min. Total proteins were separated using sodium dodecyl sulfate-polyacrylamide gel electrophoresis (SDS-PAGE) and transferred onto nitrocellulose membranes. After blocking for 1 h with 5% bovine serum albumin in Tris-buffered saline (BD Biosciences, San Diego, CA, USA) containing Tween-20 (Life Technologies, Grand Island, NY, USA) at room temperature. Membranes were incubated with primary antibody at 4° C (1 : 1000 or 1 : 5000 dilution) overnight and then incubated with secondary antibody (1 : 5000 dilution) for 1 h at room temperature. The antibodies used

to study the apoptotic signaling pathways included antibodies against Fas ligand (48 kDa), cleaved caspase-3 (17 and 19 kDa), cleaved caspase-8 (18 kDa), and cleaved caspase-9 (37 kDa), PARP (116 and 85 kDa), Bid (22 and 15 kDa), Bcl-2 (26 kDa), Bcl-xL (26 kDa), Bax (21 kDa), Bad (23 kDa), β -actin (45 kDa), phospho-Erk1/2 (42 and 44 kDa), total-Erk1/2 (42 and 44 kDa), Phospho-p38 (43 kDa), total-p38 (43 kDa), phospho-Akt (60 and 56 kDa), total Akt (62 kDa), phospho-mTOR (250 kDa), total-mTOR (250 kDa), p53(53 kDa), p21 (21 kDa), p27 (27 kDa), MMP-2 (72 and 63 kDa), and MMP-9 (92 kDa). The immunoreactivity bands were visualized using the ECL System (Amersham Biosciences, Piscataway, NJ, USA) and exposed on radiographic film.

II-10. Caspase-3/-7 activity assay

To detection of caspase-3/7 activity. NucView 488 caspase-3/-7 substrate solution (Biotium Inc., Hayward, CA, USA), FaDu cells were cultured at a density of 5×10^4 cells/mL in an 8-well chamber slide (Electron Microscopy Sciences, Hatfield, PA, USA) and allowed to attach to the well overnight. After incubation, cultured FaDu cells were treated with 0, 25, and 50 μ M coumestrol for 48 h. Replace medium with fresh medium or PBS containing 1 μ M NucView 488 substrate stock solution. Incubate cells with a substrate at room temperature for 30 min. The cells wash with PBS and observe cells by fluorescence microscopy in using filter sets for green fluorescence (excitation/emission: 485/515 nm). It was Photographed using fluorescence microscopy (Eclipse TE2000, Nikon Instruments, Melville, NY, USA).

II-11. Caspase dependent cell survival assay

The cells were plated at a density of 5×10^4 cells/mL in 96-well culture plates and allowed to attach to the well overnight. After incubation, cultured

cells were treated with 50 μ M coumestrol in presence or absence of 20 μ M caspase-3 inhibitor (Z-VAD-FMK, Enzyme Systems, Dublin, CA, USA) were incubated for 48 h at 37° C. After incubation, under the defined conditions, cell cytotoxicity was measured by MTT assay and FACS was performed.

II-12. Colony formation assay

A colony formation assay was performed to assess the survival and proliferation of FaDu cells treated with coumestrol. FaDu cells were cultured at a density of 500 cells/well in a 12-well culture plate and allowed to attach to the well overnight. After incubation cultured FaDu cells treated with 5 and 10 μ M coumestrol for 24 h and then were incubated in the culture media without coumestrol for 7 and 10 days. After that, the medium removed, and the cells were washed with PBS and fixed with 4% paraformaldehyde for 10 min at 4° C. Sequentially the colonies were stained with 0.5% crystal violet for 10 min. The colonies were washed with PBS and dried at room temperature, before being imaged by a digital camera (Nikon Instruments, Melville, NY, USA).

II-13. Migration assay

To perform the migration assay, FaDu cells cultured onto 1×10^6 cells/mL, and 70 μ L of cell suspension (35,000 cells per reservoir) added to each chamber of the insert (Ibidi Regensburg, Germany). FaDu cells were allowed to attach to the coated bottom of the dish and to reach confluency overnight. After that, the inserts removed after washing the cell patch with 2 mL of DPBS, and it replaced with 2 mL of culture medium containing treated concentration with 10 μ M coumestrol for 24 and 48 h. Wound widths were imaged and measured using an inverted microscope (Eclipse TE2000, Nikon Instruments, Melville, NY, USA).

II-14. Invasion assay

For *in vitro* invasion assays, the upper chambers of the transwell (6.5-mm transwell inserts with 8.0 μm pore size polycarbonate membrane CLS3422-48EA, Sigma Aldrich, St. Louis, MO, USA) transwell was pre-coated with 10 μL of 0.5 mg/ml extracellular matrix collagen I (Sigma-Aldrich, St. Louis, MO, USA). FaDu cells 1×10^5 cells/mL seeded onto the upper side of the transwell. After 24 h, the transwell was washed in PBS and placed into serum-free FBS growth medium. Full growth medium containing 10% FBS was added to the bottom well. After incubated at 37°C for treated concentration with 0, 5, and 10 μM coumestrol for 72 h. Remove medium from the chamber wash in PBS. The insert membranes fixed with cold methanol room temperature for 20 min remove methanol from the chamber wash twice in PBS. The FaDu cells were stained with 0.05% crystal violet in PBS for 15 min. The upper side cells on the filters removed with cotton-tipped swabs and the positively stained cells invaded to the under part of the membranes counted. Positively stained cells were imaged using an inverted microscope (Eclipse TE2000, Nikon Instruments, Melville, NY, USA). The invaded FaDu cell numbers averaged from counting numbers of five random fields.

II-15. Gelatin zymography

Gelatin zymography was performed to assess the activity of matrix metalloproteinases secreted from FaDu cells treated with coumestrol. An equal volume of conditioned media was mixed with non-reducing sample buffer (4% SDS, 0.15 M Tris pH 6.8, and 20% (v/v) glycerol containing 0.05% (w/v) bromophenol blue) and resolved on a 10% polyacrylamide gel containing copolymerized 0.2% (1 mg/mL) swine skin gelatin. After electrophoresis of the conditioned media samples, gels washed with cold PBS containing 2.5%

(v/v) Triton X-100 for 30 min and washed twice with cold PBS for 15 min. After washing, gels were incubated in the zymogram renaturing buffer (50 mM Tris-HCl (pH 7.6), 10 mM CaCl₂, 50 mM NaCl, and 0.05% Brij-35) at 37° C for 48 h. After renaturation of MMPs, gels were stained with 0.1% Coomassie brilliant blue R250. The activity revealed a clear band on a background of uniform light blue staining.

II-16. Xenograft mouse model

All animal studies have performed the protocol (CIACUC2017-A0054) approved by the Institutional Animal Care and Use Committee (IACUC) of Chosun University, Gwangju Republic of Korea. Four-week-old female nude mice (Koatec, Osan, South Korea) kept under the sterile condition of the temperature of 24 ~ 26°C and 40 ~ 60% relative humidity. FaDu cell was harvested and washed with PBS, and at a concentration of 1×10^7 cells/100 μ L were injected subcutaneously into the right and left flanks. 10 days after tumor formation coumestrol (1 mg/kg) dissolved in ethanol 5% and an equal volume of the ethanol (control) treatment by daily of oral administration. Three times per week for 3 consecutive weeks. Tumor sizes were measured weekly using a vernier caliper for 3 weeks following FaDu cell xenografting, and the formula of $A \times B^2 \times 0.52$ used. A is the longest diameter of the tumor and B is the shortest diameter of the tumor. Body weights were recorded every other day as the assessment of drug toxicity. After 19 days the mice were sacrificed, and the tumor tissues were excised and fixed in 4% paraformaldehyde and embedded in paraffin for immunohistological analysis.

II-17. Histology and immunohistochemistry

Immunohistochemistry was performed using Vectastain® ABC Kit (Vector Laboratories, Burlingame, CA, USA) tumor masses were excised, post-fixed

in 4% paraformaldehyde for 7 days, dehydrated in a series of ethanol solutions (70, 80, 90, and 100%; 2 h per step), and then submerged in xylene twice for 2 h and in paraffin twice for 2 h. Paraffin-embedded tissue blocks were prepared and cut using a microtome. The 8- μ m-thick sections placed on glass slides. The sections were deparaffinized using two changes of xylene for 3 min, rehydrated with two washes each of 100, 90, 80, and 70% ethanol for 3 min, and then rinsed with tap water for 3 min. The sections incubated at 4° C with phospho-Akt, p53 antibody overnight and incubated for 1 h at room temperature with peroxidase-conjugated goat anti-mouse antibody. Sections were subsequently counterstained using hematoxylin, transferred to the mounting reagent, and examined by microscopy.

II-18. Statistical analysis

The experimental data are presented as the mean \pm standard deviation (SD) from at least three independent experiments and were compared using analysis of variance, followed by Student's *t*-test. $p < 0.05$ and $p < 0.01$ was considered statistically significant.

III. Results

III-1. Coumestrol exerts dose-dependent cytotoxicity in FaDu cells, but not in L929.

The cytotoxicity of the compounds was assessed by using an MTT assay. As shown in Figure 2, coumestrol was not toxic to L929 treated with coumestrol at 10, 20, or 50 μ M. In contrast, the survival rate of FaDu cells significantly decreased in response to coumestrol in a time- and dose-dependent manner. As shown in Figure 3, coumestrol treatment for 24 h resulted in a viable percentage of 98.8 ± 4.3 , 83.1 ± 3.4 , and $67.9 \pm 2.6\%$, respectively, compared with the untreated controls ($100 \pm 4.9\%$) in FaDu cells. Furthermore, the relative viability of FaDu cells treated with the same concentrations of coumestrol for 48 h was 97.0 ± 3.2 , 72.5 ± 5.0 , and $39.7 \pm 2.9\%$, respectively, and 94.4 ± 6.1 , ($p < 0.01$), 70.1 ± 4.6 ($p < 0.01$), and $30.9 \pm 1.9\%$ ($p < 0.01$), respectively, after treatment for 72 h. These data demonstrated that coumestrol exerted cytotoxic effects in a time- and dose-dependent manner, specifically in FaDu cancer cells.

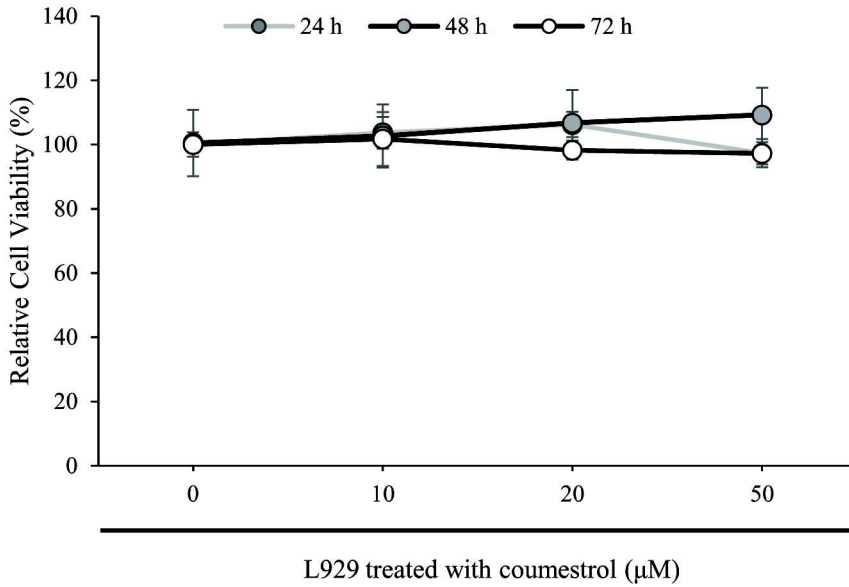


Figure 2. Coumestrol does not affect the viability of L929, used as the normal cells. L929 were cultured in 10 ~ 50 μ M coumestrol for 24, 48, and 72 h. The presented data are the mean \pm standard deviation of the results of three independent experiments (SD; $p < 0.05$ and $p < 0.01$ compared to the control).

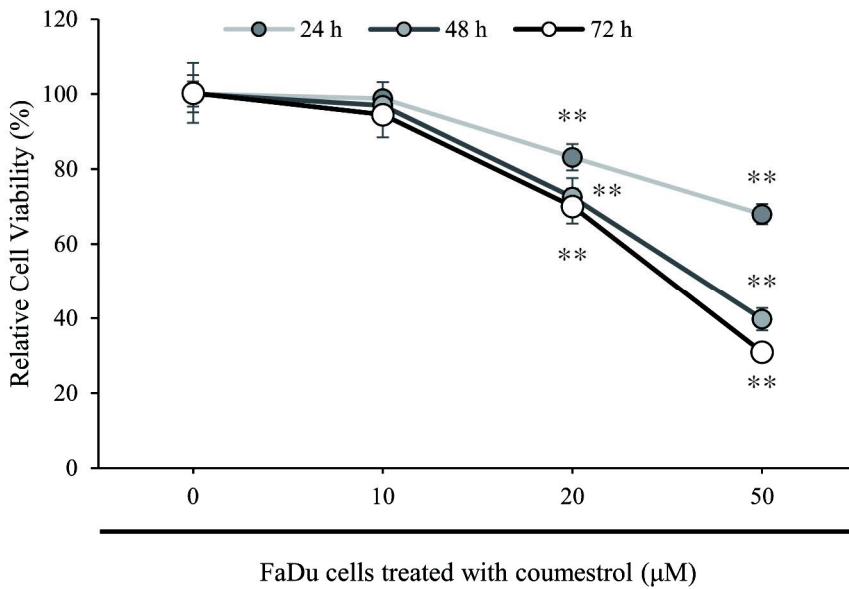


Figure 3. Coumestrol increases the cytotoxicity in FaDu cells. FaDu cells were cultured in 10 ~ 50 μ M coumestrol for 24, 48, and 72 h. The presented data are the mean \pm standard deviation of the results of three independent experiments (SD; * p < 0.05 and ** p < 0.01 compared to the control).

III-2. Coumestrol reduces the survival of FaDu cells, but did not affect L929.

To confirm the toxicity of coumestrol, the cells were seeded in 8-well chamber slides and treated with different concentrations of coumestrol (0, 25, and 50 μM) for 48 h. Cell-permeable calcein-AM was used to stain live cells with green fluorescence, and ethidium homodimer-1 was used to stain the dead cells with red fluorescence. L929 were stained as green fluorescence by membrane-permeable calcein-AM, as shown in Figure 4. The number of dead cells stained with red fluorescence by ethidium homodimer-1 was significantly increased in a dose-dependent manner in FaDu cells after treatment with coumestrol (Figure 5). The relative percentage of live FaDu cells after treatment with 20 and 50 μM coumestrol was 81.2 ± 4.6 and $64.8 \pm 9.3\%$, respectively. These data demonstrated that coumestrol induced toxicity to FaDu cells in a dose-dependent manner, but not L929 used as a normal cells.

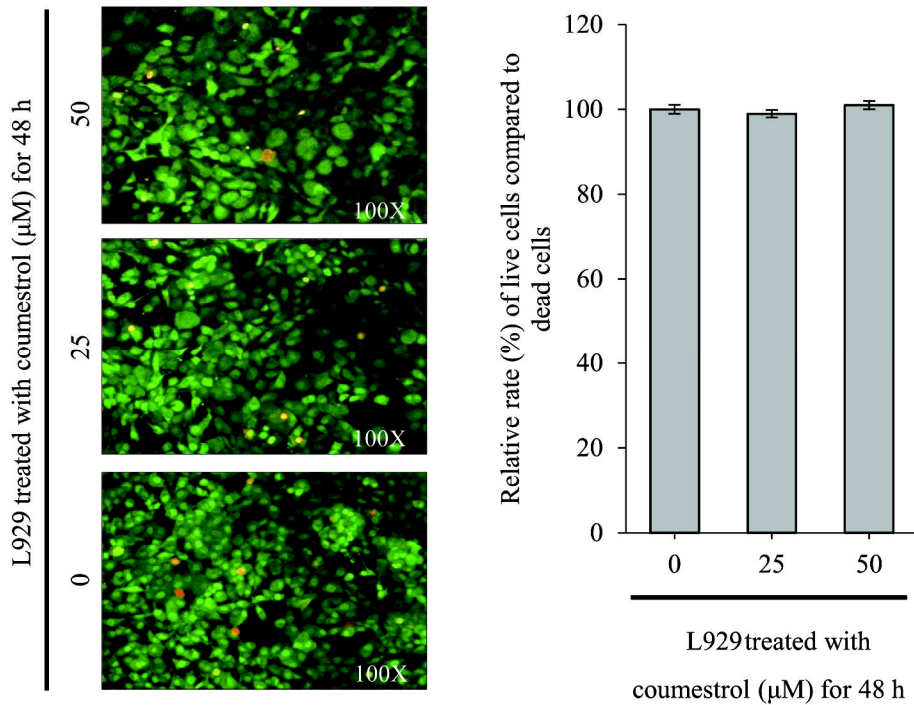


Figure 4. Coumestrol does not affect the survival of L929, used as the normal cells. The live & dead assay using green calcein-AM and ethidium homodimer-1 to stain the live cells and dead cells, respectively, was performed in L929 treated with 25 and 50 μM coumestrol for 48 h and fluorescence microscopy images of the cells were captured. (Eclipse TE2000; Nikon Instruments, Melville, NY) (SD; $p < 0.05$ and $p < 0.01$ compared to the control).

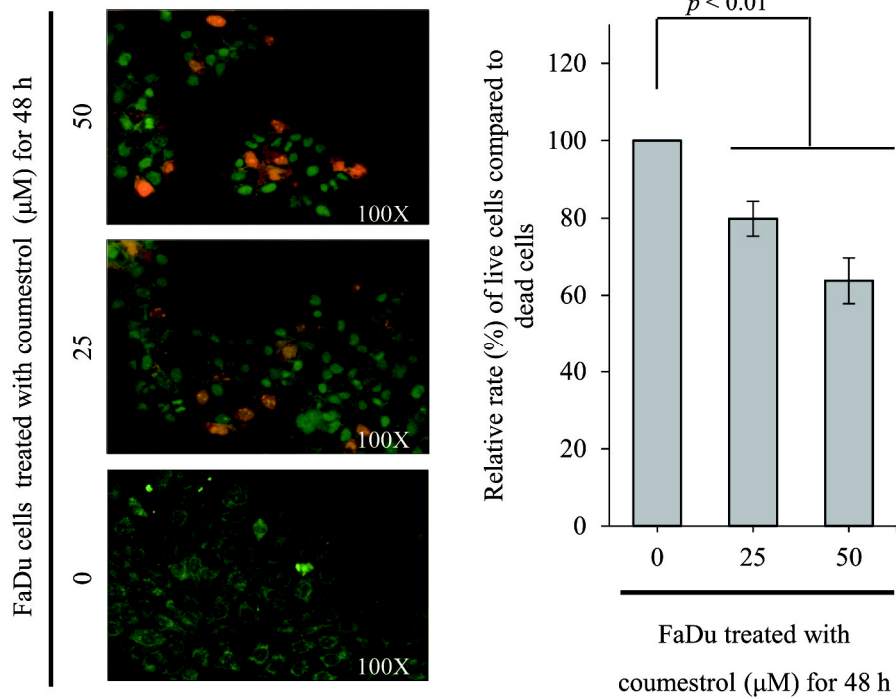


Figure 5. Coumestrol reduces the survival of FaDu cells. FaDu cells were treated with 25 and 50 μ M coumestrol for 48 h. Thereafter, the live & dead assay using green calcein-AM and ethidium homodimer-1 to stain the live cells and dead cells, respectively, was performed and fluorescence microscopy images of the cells were captured. (Eclipse TE2000; Nikon Instruments, Melville, NY) (SD; $p < 0.05$ and $p < 0.01$ compared to the control).

III-3. Formation of apoptotic bodies increases in FaDu cells treated with coumestrol.

FaDu cells were treated with 25 and 50 μ M coumestrol for 48 h and H&E staining was performed to identify the formation of apoptotic bodies and morphological alterations that are typical apoptotic phenomena. As shown in Figure 6, the number of FaDu cells was decreased by coumestrol in a dose-dependent manner. Furthermore, the number of FaDu cells with the outer membrane bulges and shrinkages that are representative morphological characteristics of apoptotic bodies was increased after treatment with coumestrol in a dose-dependent manner. These data indicated that coumestrol-induced FaDu cell death was involved with apoptosis.

FaDu cells treated with coumestrol (μM) for 48 h

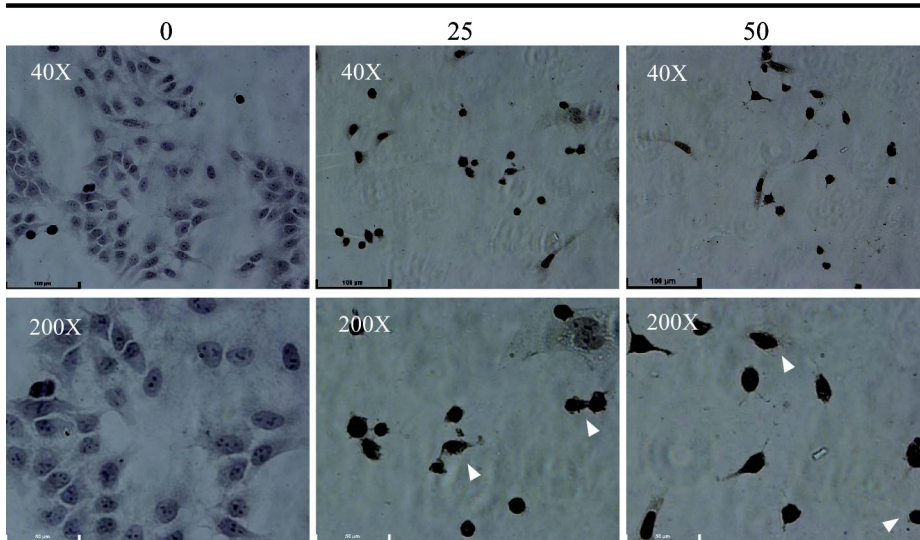


Figure 6. Coumestrol increases the formation of apoptotic bodies formation in FaDu cells. FaDu cells were treated with 25 and 50 μM coumestrol for 48 h, hematoxylin and eosin staining was performed to investigate the apoptotic body formation and morphological alterations in FaDu cells treated with coumestrol, and microscopy images of the cells were captured. The white arrows indicate morphologically altered FaDu cells (Eclipse TE2000; Nikon Instruments, Melville, NY).

III-4. Coumestrol elevates the number of FaDu cells with chromatin-condensed nuclei.

To evaluate whether coumestrol-induced FaDu cell death was involved with apoptosis, L929 and FaDu cells were treated with 25 and 50 μ M coumestrol for 48 h. Thereafter, nuclear staining using DAPI was conducted to investigate the chromatin condensation in FaDu cells. As shown in Figure 7, coumestrol did not induce the chromatin condensation in L929, which were used as normal cells. However, the number of FaDu cells with chromatin-condensed nuclei was significantly higher in the coumestrol-treated cells than in the untreated cells. These data indicated that coumestrol-induced FaDu cell death was mediated through the apoptotic signaling pathway.

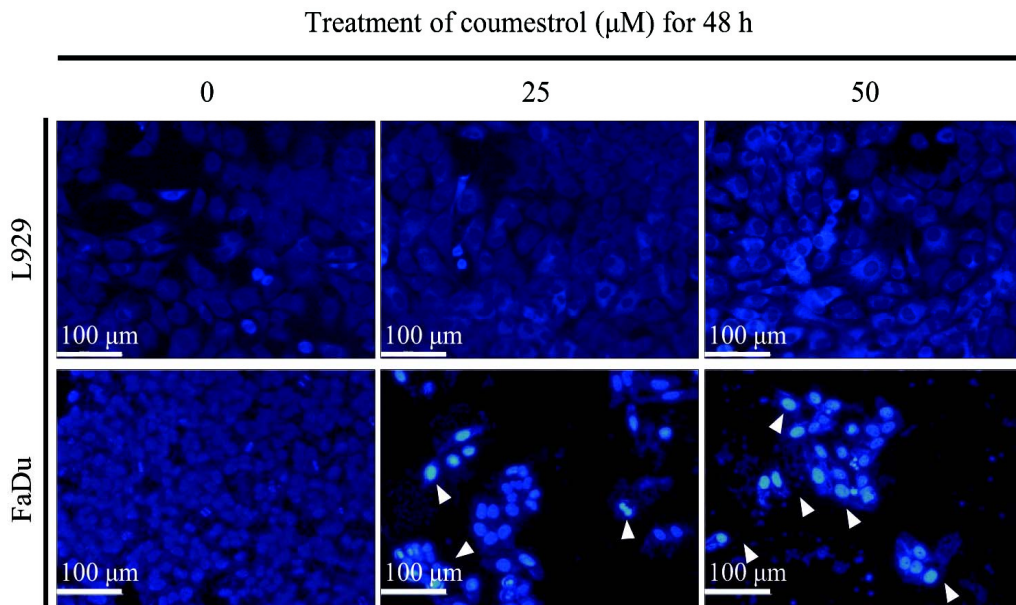


Figure 7. Coumestrol increases the number of FaDu cells with chromatin-condensed nuclei. FaDu cells were treated with 25 and 50 μM coumestrol for 48 h. Thereafter, nuclear staining using DAPI was performed to observe the nucleus condensation and fluorescence microscopy images of the cells were captured. The white arrows indicate the cells with chromatin-condensed nuclei (Eclipse TE2000; Nikon Instruments, Melville, NY).

III-5. Coumestrol induces the DNA fragmentation in FaDu cells.

To elucidate whether coumestrol induced DNA fragmentation, which is a representative apoptotic phenomenon, FaDu cells were treated with 25 and 50 μ M coumestrol for 48 h. Thereafter, total DNA was isolated and DNA fragmentation was investigated by using agarose gel electrophoresis. As shown in Figure 8, coumestrol significantly increased DNA fragmentation in FaDu cells in a dose-dependent manner compared with the untreated control cells. These data were consistent with the suggestion that coumestrol-induced FaDu cell death was mediated through the cellular apoptosis.

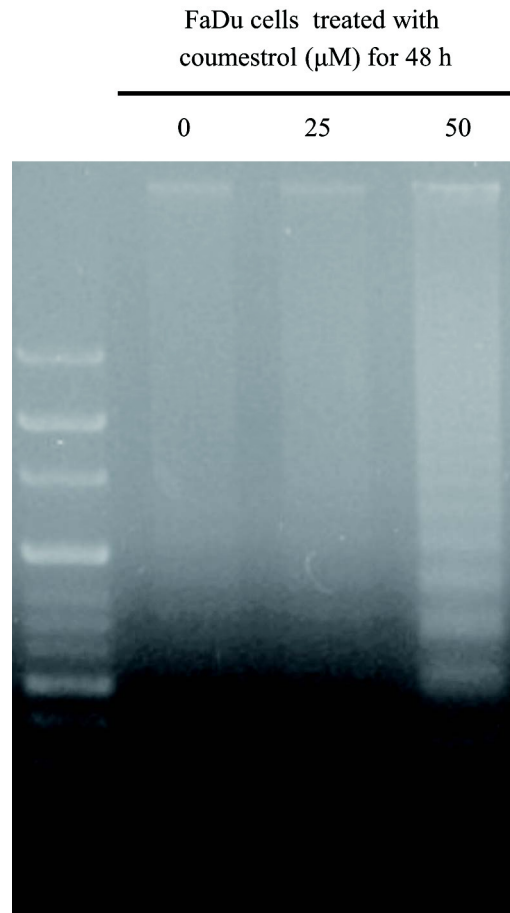


Figure 8. DNA fragmentation dose-dependently increases in FaDu cells treated with coumestrol. FaDu cells were treated with 25 and 50 μM coumestrol for 48 h. Thereafter, total DNA was isolated and electrophoresed on 1% agarose gel to observe the DNA fragmentation.

III-6. Coumestrol increases the proportion of apoptotic FaDu cells.

To confirm that coumestrol-induced FaDu cell apoptosis, FaDu cells were treated with 25 and 50 μ M coumestrol for 48 h. Thereafter, FACS analysis was performed using annexin V-FITC and PI, as shown in Figure 9. The total population of apoptotic cells was significantly increased by 27.9 and 49.7% in FaDu cells treated with 25 and 50 μ M coumestrol for 48 h, respectively, compared with the untreated controls (9.8%). These data indicated that coumestrol increased the proportion of apoptotic FaDu cells. Furthermore, these data were consistent with the indication that coumestrol induced the death of FaDu cells through the apoptotic cellular pathways.

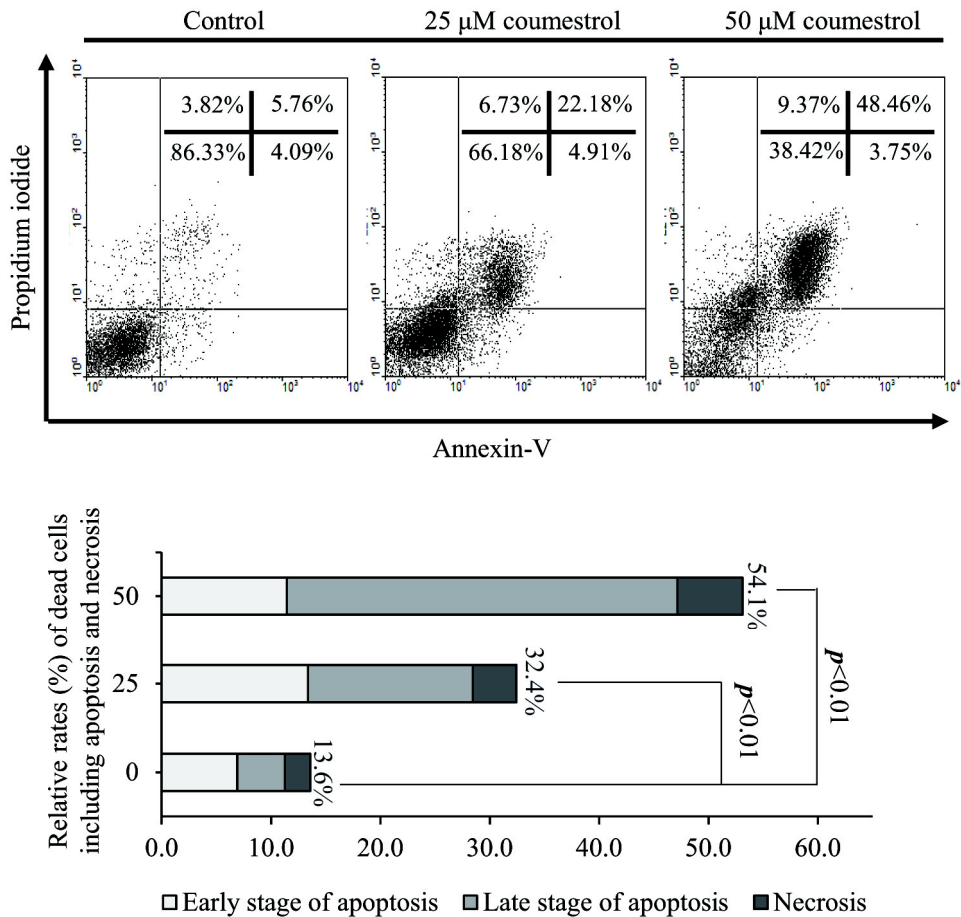


Figure 9. Coumestrol dose-dependently increases the proportion of FaDu cells undergoing apoptosis. FaDu cells were treated with 25 and 50 μ M coumestrol for 48 h. Thereafter, FACS analysis using annexin V and propidium iodide staining was performed to confirm coumestrol-induced apoptosis in FaDu cells. Black bar, necrosis; dark grey, late-stage apoptosis; light grey, early stage apoptosis (SD; $p < 0.05$ and $p < 0.01$ compared to the control).

III-7. Coumestrol-induced FaDu cell death is mediated by apoptosis through the death receptor-mediated (extrinsic) and mitochondria-dependent (intrinsic) pathways.

To verify the coumestrol-induced pathway of cellular apoptosis, FaDu cells were treated with 25 and 50 μ M coumestrol for 48 h. Thereafter, FaDu cells were harvested, lysed in cell lysis buffer, and analyzed by western blotting. As shown in Figure 10, the expression of FasL, a representative death ligand associated with death receptor-mediated (extrinsic) apoptosis, was significantly increased in FaDu cells treated with coumestrol in a dose-dependent manner. Subsequently, the expression of cleaved caspase-8 was significantly increased through the cleavage of pro-caspase-8, a downstream target pro-apoptotic factor of FasL. These data suggested that coumestrol-induced FaDu cell death was involved with death receptor-mediated (extrinsic) apoptosis, which is triggered by death ligand FasL. Cleaved caspase-8 may initiate mitochondrial-dependent (intrinsic) apoptosis through the cleavage of Bid to tBid. Hence, the alteration of the anti-apoptotic and pro-apoptotic factors associated with mitochondrial-dependent apoptosis was investigated, as shown in Figure 11. The expression of anti-apoptotic factors, such as Bcl-2 and Bcl-xL, was decreased in FaDu cells treated with coumestrol in a dose-dependent manner, whereas coumestrol increased the expression of pro-apoptotic factors, such as tBid, Bax, and Bad, which are closely associated with a decrease in mitochondrial membrane potential. Subsequently, the expression of cleaved caspase-9 was dose-dependently increased by coumestrol through the cleavage of pro-caspase-9 by cytochrome c released from mitochondria, which decreased the mitochondrial membrane potential of FaDu cells. These data suggested that coumestrol-induced FaDu cell death was mediated by the mitochondria.

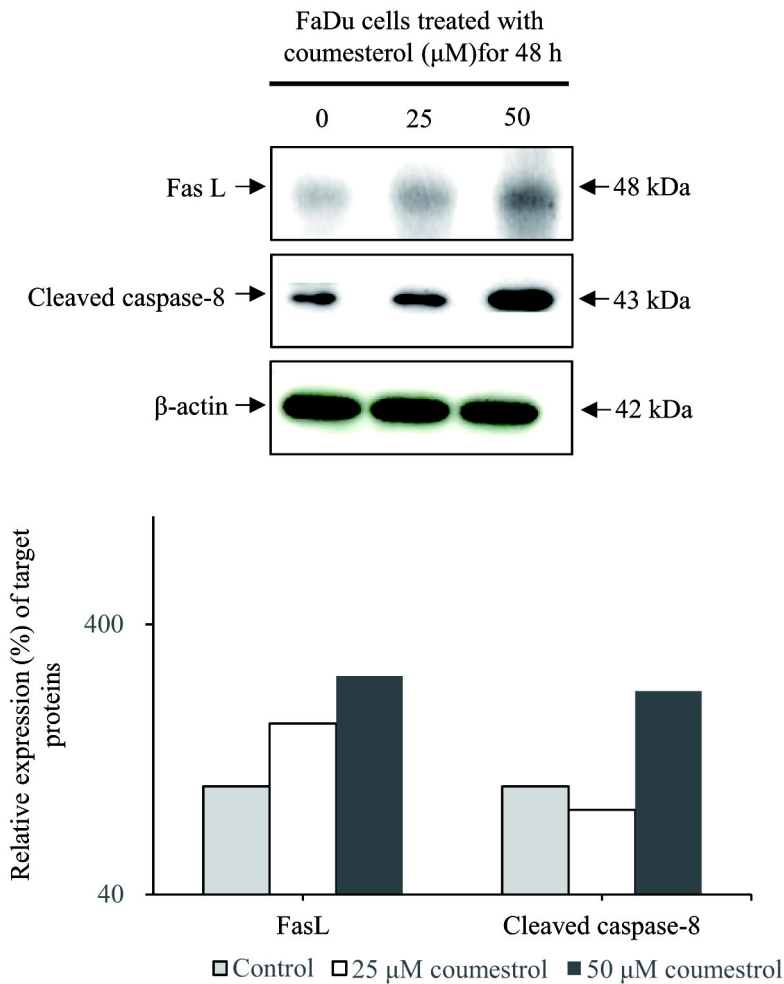


Figure 10. Cleaved caspase-8, a death receptor-mediated (extrinsic) pro-apoptotic factor, is dose-dependently increased by the expression of FasL in FaDu cells treated with coumestrol. FaDu cells were treated with coumestrol for 48 h. Thereafter, total proteins were extracted and identified by western blotting for antibodies associated with extrinsic apoptosis such as FasL and caspase-8. Densitometry analysis of the western blot was computed by ImageJ software to verify changes in the expression of pro-apoptotic factors associated with the extrinsic apoptosis pathway.

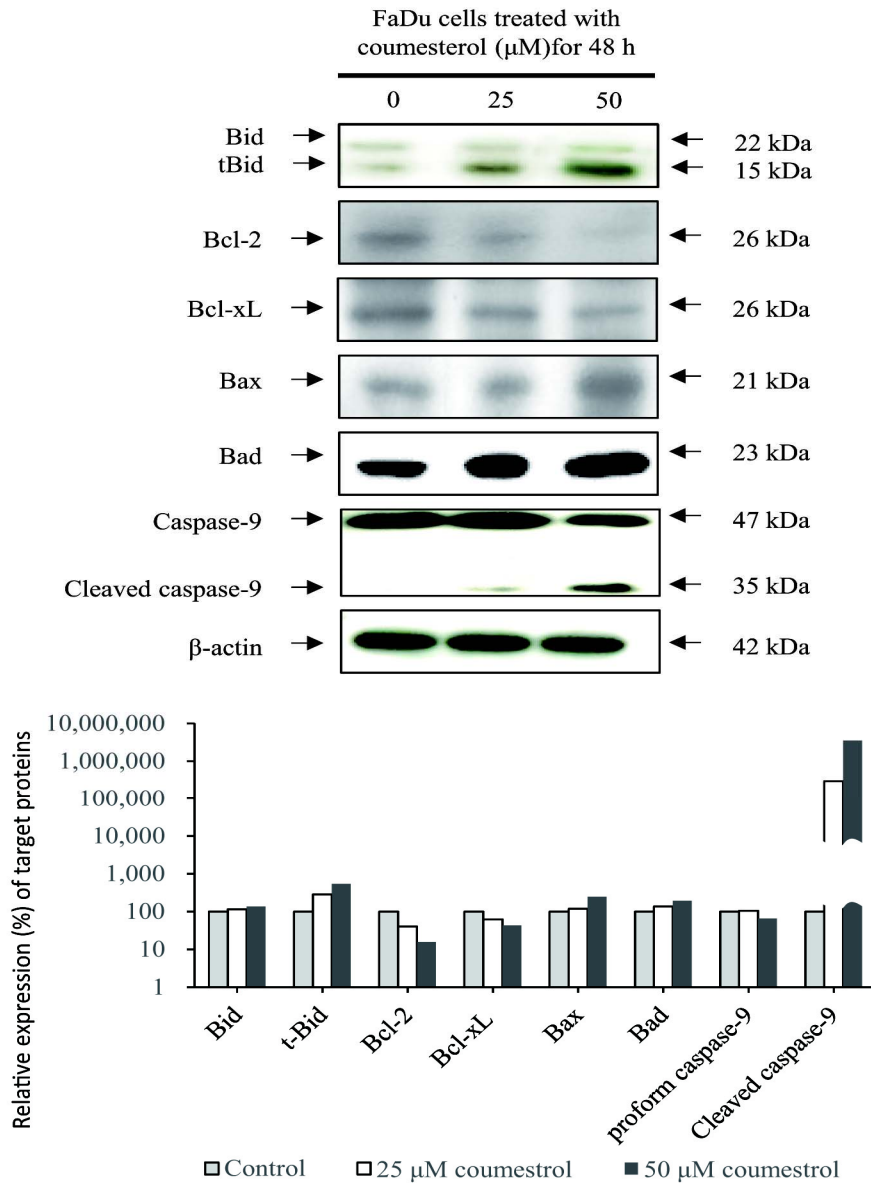


Figure 11. Mitochondrial-dependent intrinsic apoptosis is involved with FaDu cell death mediated by coumestrol. Coumestrol induces mitochondrial-dependent intrinsic apoptosis through the upregulation of pro-apoptotic factors and the downregulation of anti-apoptotic factors in FaDu cells.

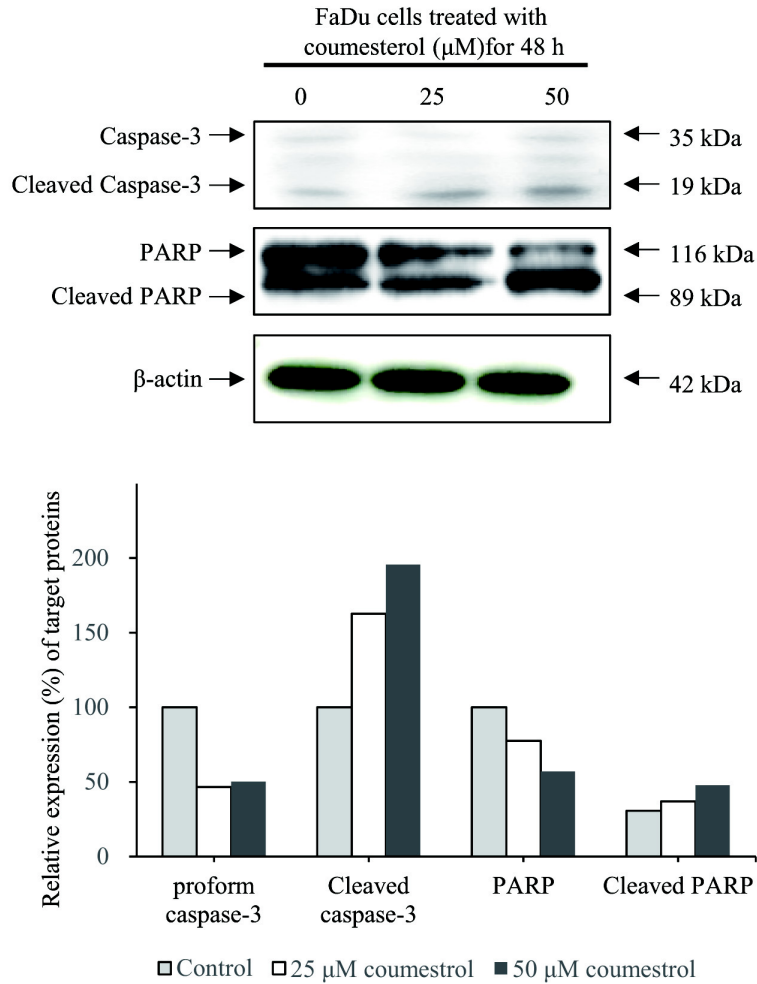


Figure 12. Coumestrol induces FaDu cell death through the activation of caspase-3 and poly(ADP ribose)polymerase (PARP). Coumestrol increases the expression of cleaved caspase-3 and cleaved PARP, which are downstream apoptotic target molecules of death receptor-mediated (extrinsic) and mitochondrial-dependent (intrinsic) apoptosis pathways, in FaDu cells.

To verify the cleavage of pro-caspase-3, which is a downstream target pro-apoptotic factor of cleaved caspase-8 and cleaved caspase-9 located in the death receptor-mediated (extrinsic) and mitochondrial-dependent (intrinsic) apoptotic pathways, respectively, changes in the expression of caspase-3 and its downstream target molecule, PARP, were investigated, as shown in Figure 12. The expression of cleaved caspase-3 and its downstream target molecule, PARP, was increased in a dose-dependent manner in FaDu cells treated with coumestrol. These data consistently demonstrated that coumestrol induced the apoptosis of FaDu cells through both the death receptor-mediated (extrinsic) and mitochondrial-dependent (intrinsic) pathways.

III-8. Coumestrol-induced FaDu cell apoptosis is dependent on the activation of caspase-3.

To verify whether coumestrol induced the apoptosis of FaDu cells through the activation of caspase-3, FaDu cells were treated with 25 and 50 μ M coumestrol for 48 h. Subsequently, a caspase-3/-7 activity assay, using a cell-permeable caspase-3/-7 substrate solution, was performed to verify the activation of caspase-3 in FaDu cells treated with coumestrol. As shown in Figure 13, the number of FaDu cells with green fluorescence that resulted from the cleavage of the cell permeable fluorogenic substrate by cleaved caspase-3, was significantly increased in a dose-dependent manner by the presence of coumestrol compared with that the control sample. These data suggested that coumestrol-induced FaDu cell apoptosis was dependent on the activation of caspase-3. Hence, to verify that coumestrol-induced FaDu cell apoptosis was dependent on the activation of caspase-3, FaDu cells were treated with 50 μ M coumestrol in the presence or absence of 20 μ M Z-VAD-FMK for 48 h. Subsequently, an MTT assay (Figure 14A) and western blotting (Figure 14B) were performed. The MTT assay showed that coumestrol decreased the survival rate of FaDu cells, and that the effects of coumestrol were rescued by 20 μ M Z-VAD-FMK. These data consistently demonstrated that coumestrol-induced apoptosis of FaDu cells was dependent on the activation of caspases. Moreover, western blotting was conducted to verify the changes in caspase-3 and its downstream target molecule PARP in FaDu cells treated with coumestrol and 20 μ M Z-VAD-FMK. Z-VAD-FMK (20 μ M) was shown to antagonize the coumestrol-induced expression of cleaved caspase-3 and cleaved PARP in FaDu cells. To confirm that the coumestrol-induced apoptosis of FaDu cells was dependent on the activation of caspases, FACS analysis was performed. FaDu cells were stimulated with 50 μ M coumestrol in the presence or absence of 20 μ M Z-VAD-FMK for 48 h, as shown in Figure 15. The relative proportion of apoptotic cells was

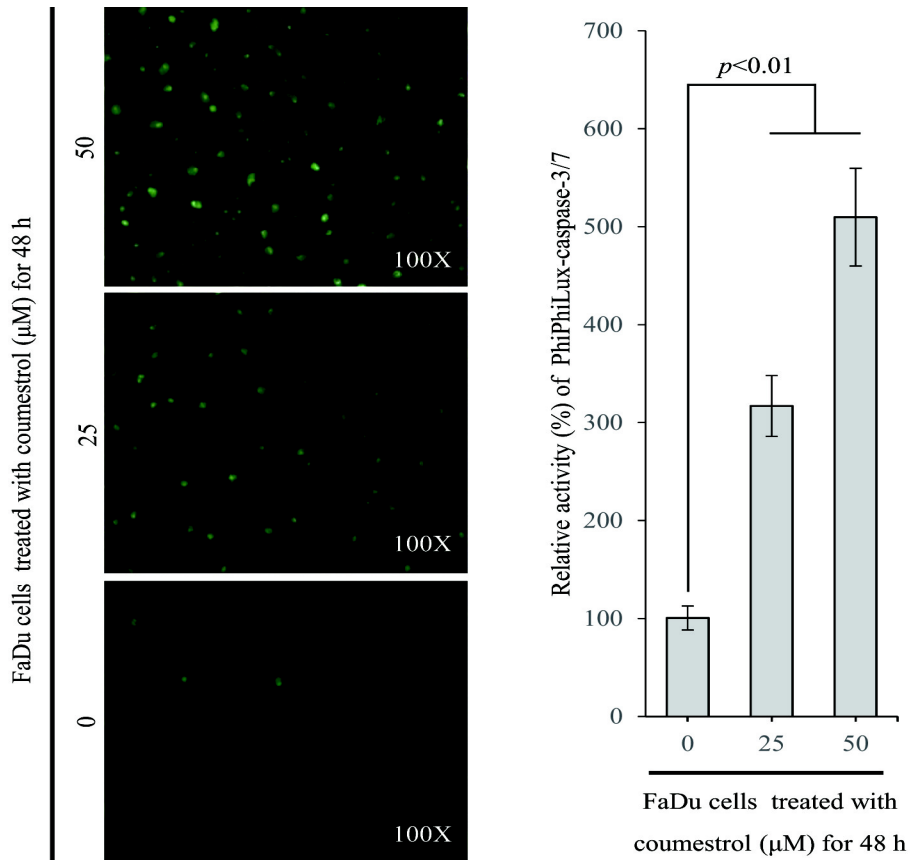
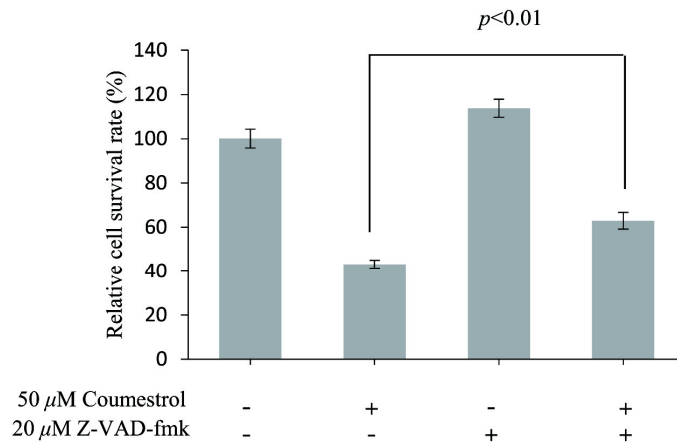


Figure 13. The activity of caspase-3/-7 is dose-dependently upregulated in FaDu cells treated with coumestrol. The caspase-3/-7 activity assay using the cell-permeable fluorogenic substrate caspase-3/-7 substrate solution (Biotium Inc., Hayward, CA, USA), was performed to verify the activation of caspase-3 in FaDu cells treated with coumestrol and fluorescence microscopy images of the cells were captured (Eclipse TE2000; Nikon Instruments, Melville, NY).

A.



B.

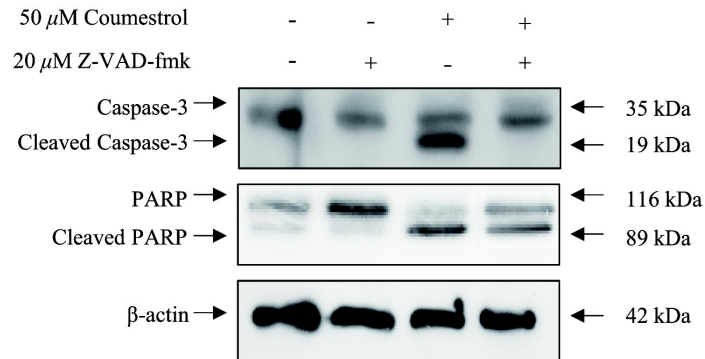


Figure 14. Coumestrol-induced FaDu cell apoptosis is dependent on caspase activation. FaDu cells were cultured with coumestrol in the presence or absence of Z-VAD-FMK. Cell cytotoxicity using an MTT assay (A) and western blotting for caspase-3 and PARP (B) were performed to determine whether coumestrol-induced FaDu cell death was caspase-dependent (SD; $p < 0.05$ and $p < 0.01$ compared to the control).

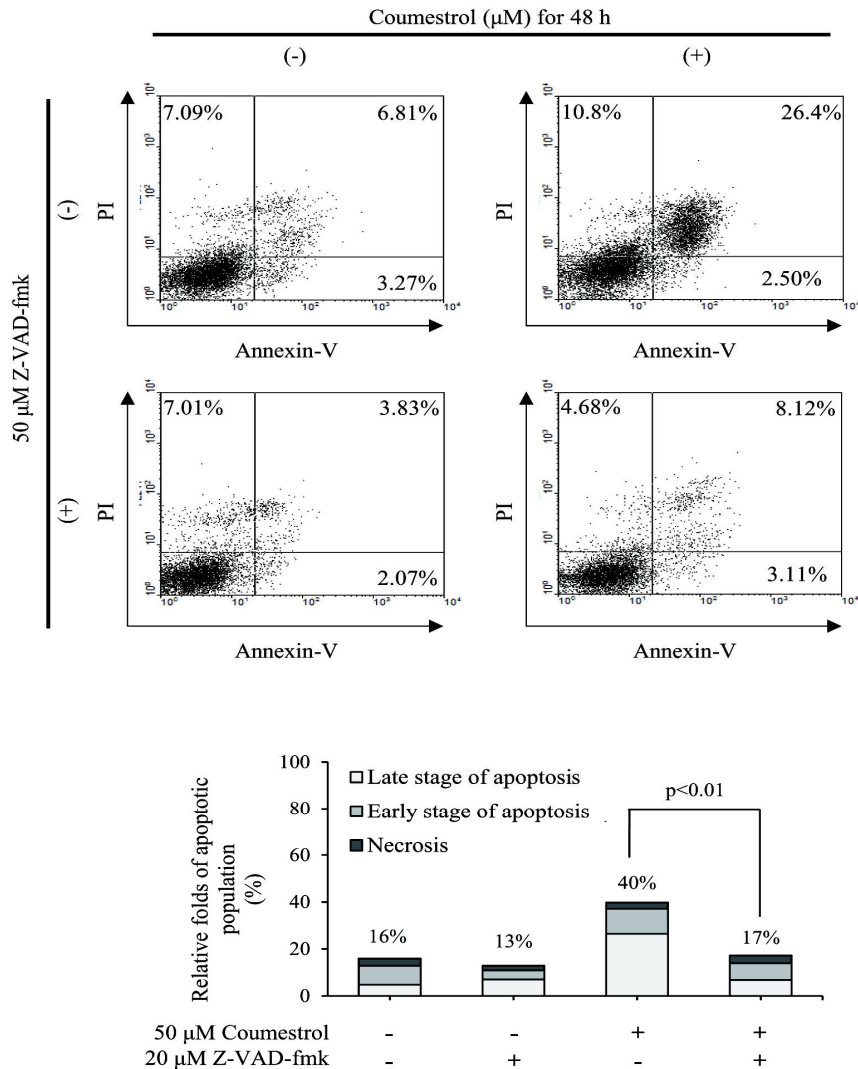


Figure 15. Pan-caspase inhibitor, Z-VAD-FMK suppresses apoptotic cell death in FaDu cells treated with coumestrol. FaDu cells were treated with 50 μM coumestrol in the presence or absence of 20 μM Z-VAD-FMK. FACS analysis was performed to verify the caspase-dependent coumestrol induction of FaDu cell death (SD; $p < 0.05$ and $p < 0.01$ compared to the control).

measured to be approximately 40% in FaDu cells treated with coumestrol. However, in the presence of 20 μ M Z-VAD-FMK, the proportion of apoptotic cells was increased by approximately 17% in FaDu cells treated with coumestrol. These data demonstrated that Z-VAD-FMK rescued the viability of FaDu cells treated with coumestrol. Furthermore, these data indicated that coumestrol-induced apoptosis of FaDu cells was dependent on the activation of caspases.

III-9. Coumestrol suppresses colony formation in FaDu cells.

The colony formation assay was performed to determine the effects of coumestrol on the proliferation of FaDu cells. FaDu cells treated with 5 and 10 μM coumestrol for 24 h and were then incubated in the culture media without coumestrol for 7 and 10 days. Thereafter, the formed colonies of FaDu cells were stained by crystal violet and counted. The number of colonies in the untreated FaDu cells (control) was 177 ± 1.4 colonies; in contrast, the number of colonies was 137 ± 3.5 and 113 ± 4.9 colonies in FaDu cells treated with 5 and 10 μM coumestrol for 7 days, respectively. After 10 days, 289 ± 2.1 colonies were counted in the control; in contrast, 258 ± 10 and 170 ± 2.1 colonies were counted in FaDu cells treated with 5 and 10 μM coumestrol for 10 days, respectively. As shown in Figure 16, coumestrol suppressed colony formation in FaDu cells in a dose-dependent manner. These data demonstrated the antitumor effects of coumestrol, suppressing colony formation through the inhibition of the proliferation of FaDu cells.

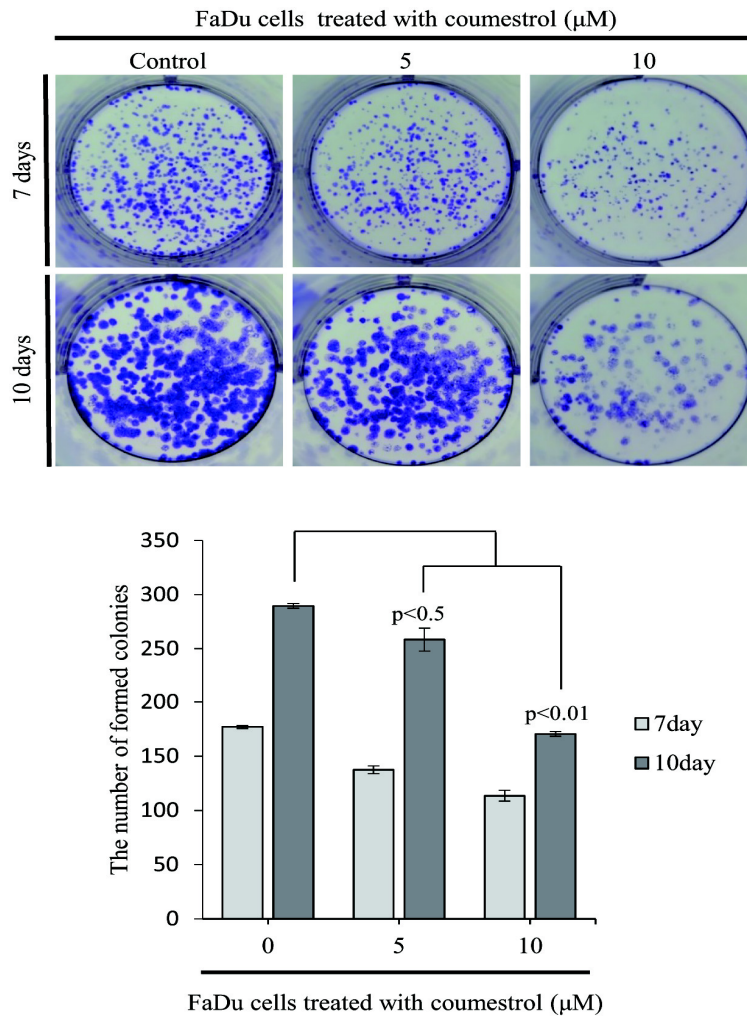


Figure 16. Coumestrol suppresses colony formation through the attenuation of FaDu cell proliferation. The colony formation assay was performed in FaDu cells treated with 5 and 10 μM coumestrol for 24 h and then incubated in culture media without coumestrol for 7 and 10 days. Crystal violet staining was performed to identify colony formation (SD; $p < 0.05$ and $p < 0.01$ compared to the control).

III-10. Coumestrol attenuates effectively the migration of FaDu cell.

To observe the effects of coumestrol on FaDu cell migration, cells were photographed after 24 and 48 h of treatment. Coumestrol effectively inhibited migration in a concentration-dependent manner compared with that in the untreated control cells. The migration distance in control FaDu cells was $99.2 \pm 2.5 \mu\text{m}$; in contrast, the migration distance in FaDu cells treated with $10 \mu\text{M}$ coumestrol for 24 h was $152.3 \pm 10.9 \mu\text{m}$. After 48 h, the migration distance was $40.4 \pm 8.2 \mu\text{m}$ in control FaDu cells and $101.6 \pm 1.7 \mu\text{m}$ in FaDu cells treated with $10 \mu\text{M}$ coumestrol. As shown in Figure 17, the migration distance was reduced in FaDu cells. However, the migration of FaDu cells was effectively attenuated by coumestrol compared with the untreated control. Collectively, these data suggested that coumestrol attenuated the migration of FaDu cells. (Eclipse TE2000; Nikon Instruments, Melville, NY). (SD; $p < 0.05$ and $p < 0.01$ compared to the control).

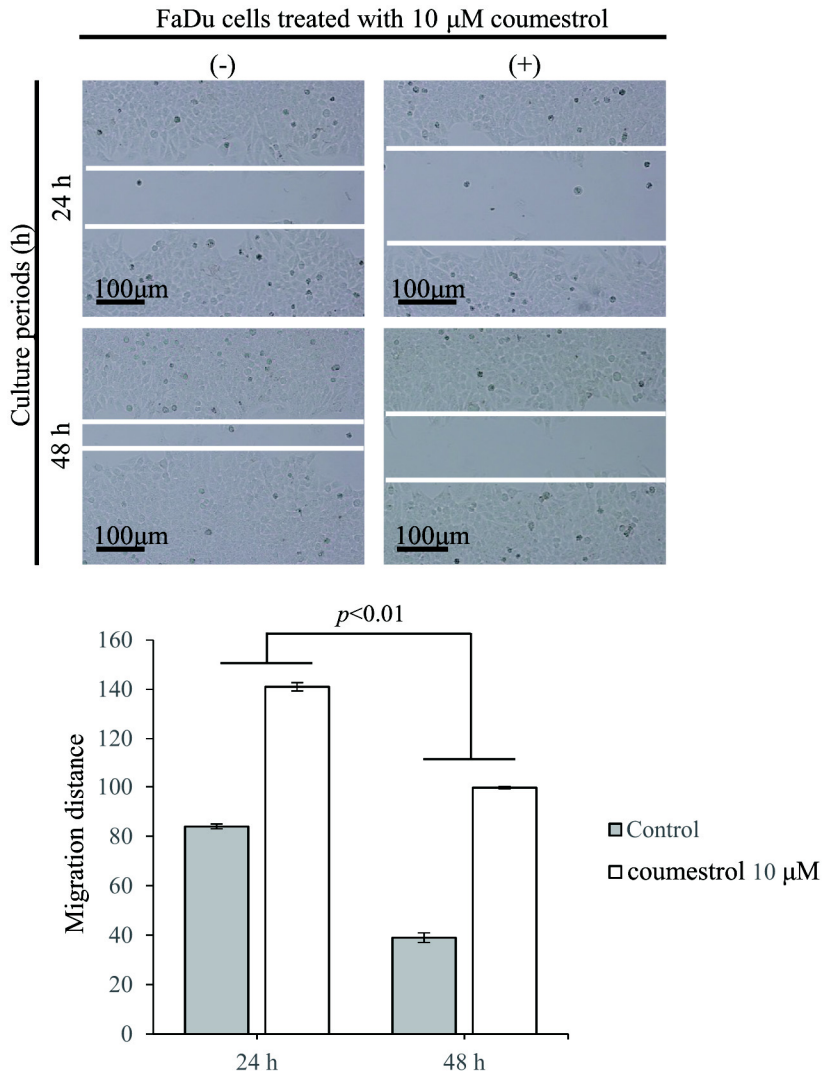


Figure 17. Migration decreases in FaDu cells treated with coumestrol. FaDu cells were treated with coumestrol for 24 and 48 h to verify whether coumestrol effectively suppresses the migration compared with the untreated control and fluorescence microscopy images of the cells were captured.

III-11. Coumestrol suppresses the invasion of FaDu cells.

The chamber insert apparatus was used to measure cell invasion. Medium containing 10% FBS was added to the lower chamber as a chemo-attractant. FaDu cells were treated with 5 and 10 μ M coumestrol for 72 h. Thereafter, crystal violet staining was used to verify the invasion of FaDu cells. As shown in Figure 18, the percentage of invading FaDu cells was 78.7 ± 3.1 and $58.9 \pm 1.1\%$ upon treatment with 5 and 10 μ M coumestrol for 72 h, respectively, compared with that of the control cells. Coumestrol inhibited the invasion of FaDu cells. Therefore, these data suggested that coumestrol exerts antitumor effects through the suppression of the invasion of FaDu cells.

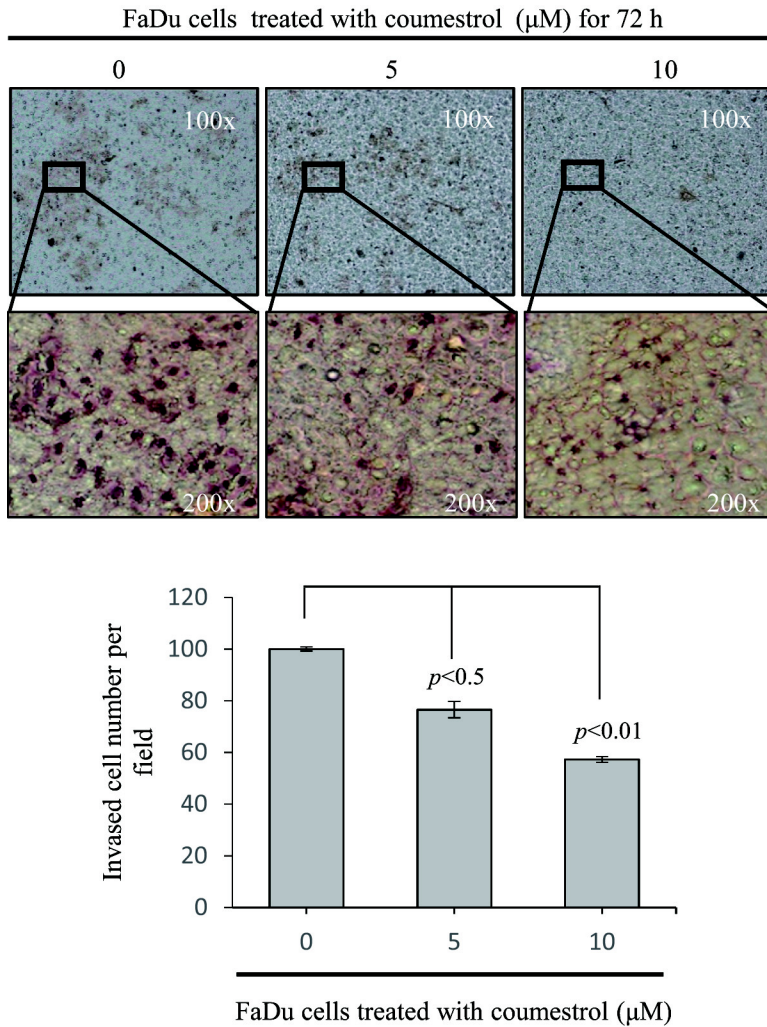
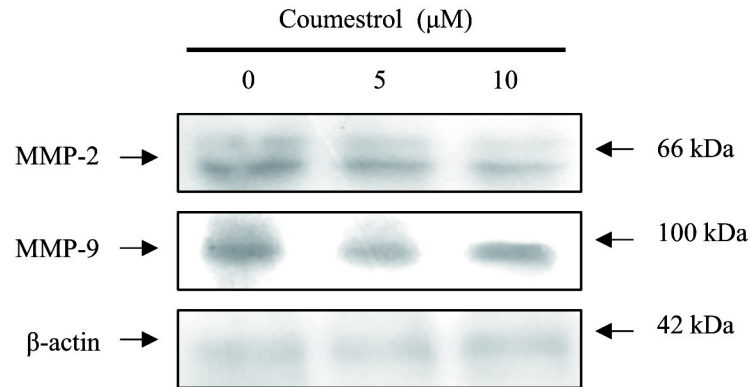


Figure 18. Coumestrol suppresses the invasion of FaDu cells. FaDu cells were treated with coumestrol for 72 h to verify if coumestrol suppresses invasion, and fluorescence microscopy images of the cells were captured. (Eclipse TE2000; Nikon Instruments, Melville, NY). (SD; $p < 0.05$ and $p < 0.01$ compared to the control).

III-12. Downstream molecules affect the metastatic suppression of coumestrol in FaDu cells.

To identify the signaling molecules involved in the effect of coumestrol on the migration and invasion of FaDu cells, FaDu cells were stimulated with 5 and 10 μ M coumestrol for 48 h. Subsequently, western blotting and gelatin zymography were performed to verify the expression and activity of MMP-2 and MMP-9 in the conditioned media of FaDu cells treated with coumestrol. The expression of MMP-2 and MMP-9 gradually decreased in FaDu cells treated with coumestrol in a dose-dependent manner (Figure 19A). Furthermore, similar to their expression, the activation of MMPs was significantly suppressed in FaDu cells treated with coumestrol (Figure 19B). These data indicated that coumestrol suppressed the proliferation, wounding migration, and invasion of FaDu cells through the downregulation of the expression and activation of MMPs.

A.



B.

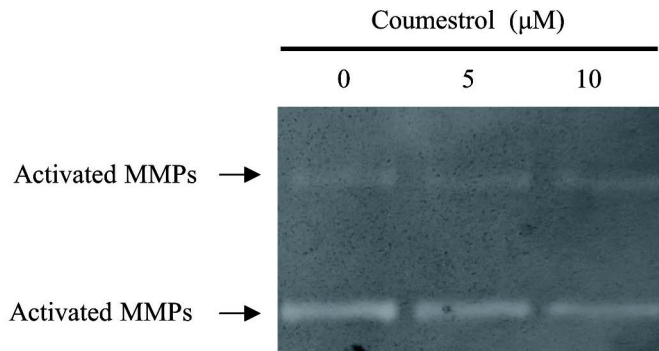


Figure 19. The expression and activity of MMP-2 and MMP-9 decreases in FaDu cells treated with coumestrol. Western blotting (A) and gelatin zymography (B) were performed to verify the changes in factors associated with the migration and proliferation of FaDu cells.

III-13. Coumestrol-induced antitumor effects are mediated by alterations in the PI3K/Akt-mTOR axis and MAPK cellular signaling pathways in FaDu cells.

To investigate the cellular signal transduction pathways associated with the coumestrol-induced antitumor effects in FaDu cells, the alteration of cellular signaling molecules, such as the PI3K/Akt-mTOR axis, cell arrest markers such as p21 and p27, and mitogen-activated protein kinases, were observed (Figures 20-22). The changes in Akt, which is a serine/threonine-specific protein kinase associated with cell proliferation and cell survival, were observed by using western blot, as shown in Figure 20. The phosphorylation of Akt and its downstream target, mTOR, was dose-dependently decreased in FaDu cells treated with 10, 25, and 50 μ M coumestrol. Subsequently, the expression of p53, a known tumor suppressor, was increased in a dose-dependent manner in FaDu cells treated with coumestrol. These data indicated that coumestrol-induced antitumor effects, including apoptosis, the suppression of colony formation, and the inhibition of invasion and wounding migration, were mediated by the suppression of FaDu cell proliferation through the modulation of the PI3K/Akt-mTOR axis and the expression of tumor suppressor p53. Furthermore, cell division was powerfully regulated by cell-cycle inhibitors, such as the p21 and p27^{Cip/Kip} proteins. Therefore, western blotting was performed to determine whether coumestrol induced the expression of p21 and p27 in FaDu cells (Figure 21). The expression of p21 and p27 was gradually decreased in FaDu cells treated with 25 and 50 μ M coumestrol for 48 h. These data suggested that coumestrol may induce the arrest of FaDu cells through the upregulation of p21 and p27, which act as cyclin-dependent kinases. Next, western blotting was performed to verify the alteration of mitogen-activated protein kinases in FaDu cells treated with coumestrol (Figure 22). FaDu cells were treated with 50 μ M coumestrol for 15, 30, and 60 min. Thereafter, the proteins were extracted from harvested FaDu cells and were electrophoresed on 10% SDS-PAGE gels prior to protein

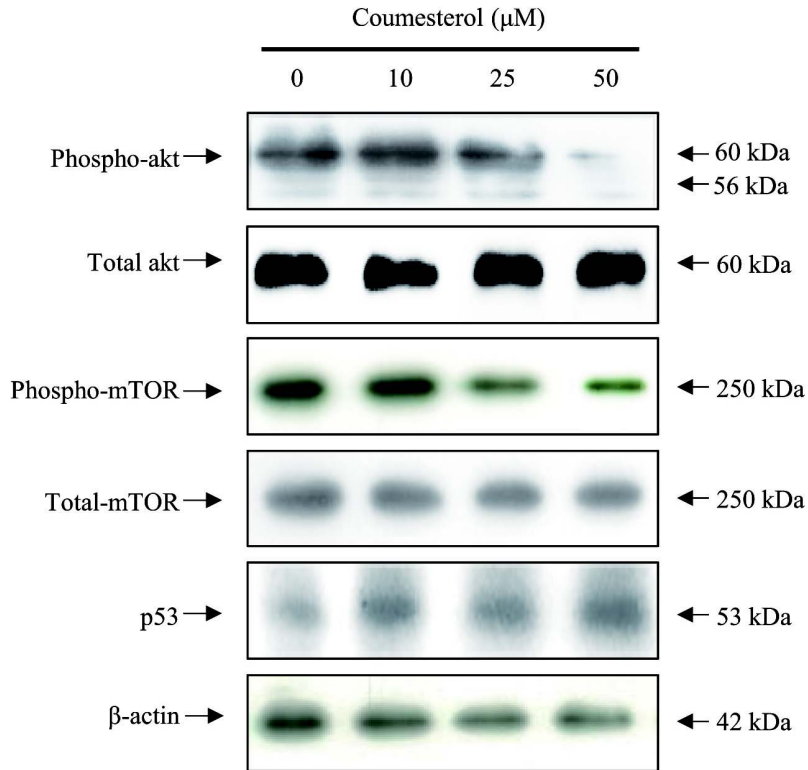


Figure 20. Coumestrol suppresses the phosphorylation of Akt and its downstream factor mTOR, but increases the tumor suppressor p53 in FaDu cells. FaDu cells were treated with 10, 25, and 50 μM coumestrol for 48 h. Western blotting was performed to investigate the changes in Akt, mTOR, and p53. The immunoreactivity bands were visualized by using the ECL system and exposed on radiographic film.

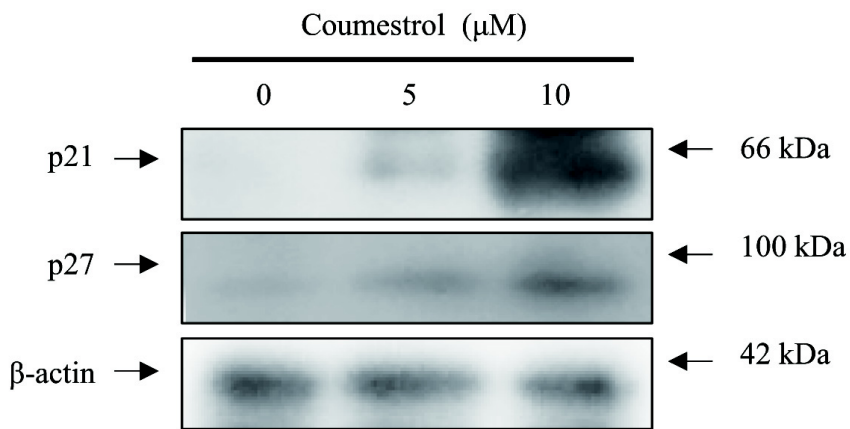


Figure 21. Coumestrol increases the cell-cycle arrest markers p21 and p27 in FaDu cells. FaDu cells were treated with 5 and 10 μM of coumestrol for 48 h. Thereafter, western blotting for cyclin-dependent kinase inhibitors such as the p21 and p27 proteins was performed to verify their expression.

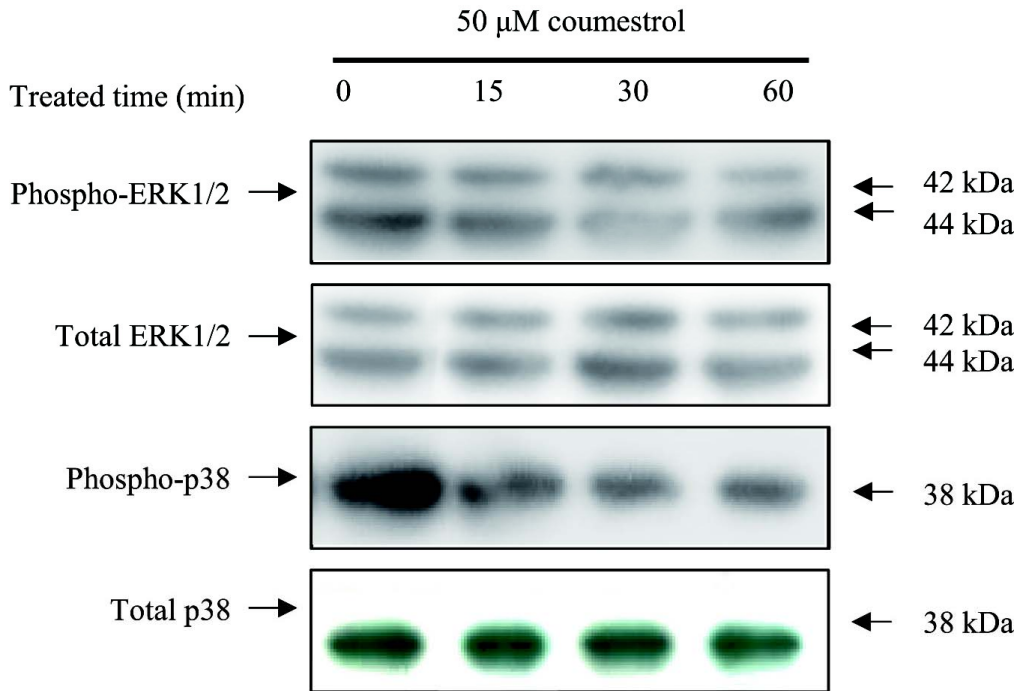


Figure 22. Coumestrol-induced cell anti-proliferation and apoptosis is mediated by the suppression of MAPK in FaDu cells. Coumestrol-induced cell anti-proliferation and apoptosis is mediated by the suppression of MAPK in FaDu cells.

identification by western blotting. As shown in Figure 22, the phosphorylation of ERK1/2 and p38 were time-dependently suppressed in FaDu cells treated with 50 μ M coumestrol. These data suggested that coumestrol-induced antitumor effects were closely associated or regulated by the alteration of the MAPK cellular signaling pathway in FaDu cells.

III-14. Antitumor effects of coumestrol in the animals xenografted with FaDu cells.

To assess the effects of coumestrol on FaDu tumor growth in vivo, FaDu cells were xenografted into experimental animals (mice) and the resulting tumor sizes and body weights were measured weekly for up to 3 weeks. As shown in Figure 23, there was no obvious loss of body weight in xenografted animals for 3 weeks, which indicated that coumestrol was well tolerated. The tumor volumes and growth were significantly lower in mice that were administered coumestrol than those in the control group (Figure 23B-23D). Furthermore, immunohistochemical analysis of the tumors showed that the phosphorylation of Akt was significantly downregulated in coumestrol-treated tumors compared with control tumors. In contrast, the expression of p53 was markedly increased in coumestrol-treated tumors compared with the control (Figure 24). Collectively, these data consistently indicated that coumestrol suppressed tumor formation through the modulation of the Akt signaling pathway in animals xenografted with FaDu cells.

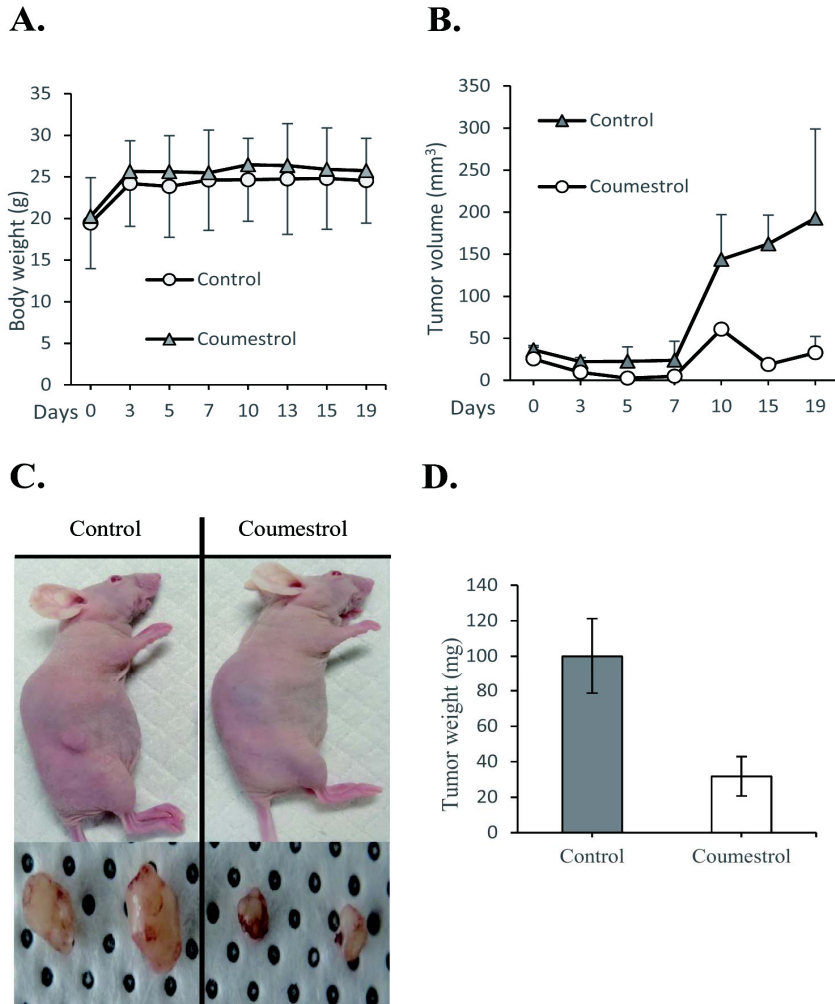


Figure 23. Coumestrol inhibits the growth of FaDu tumors in a xenograft animal model. Coumestrol (1 mg/kg) and vehicle were orally administered to the experimental and control groups of animals, respectively, three times per week for 3 weeks consecutively. The tumor sizes and body weights were measured for up to 3 weeks. (A) Coumestrol (1 mg/kg) does not affect animal body weight. (B) Coumestrol significantly reduces tumor growth in the FaDu xenograft animal model. (C) Coumestrol (1 mg/kg) significantly inhibits tumor size in animals. (D) Coumestrol significantly reduces tumor weight in the FaDu xenograft animal model.

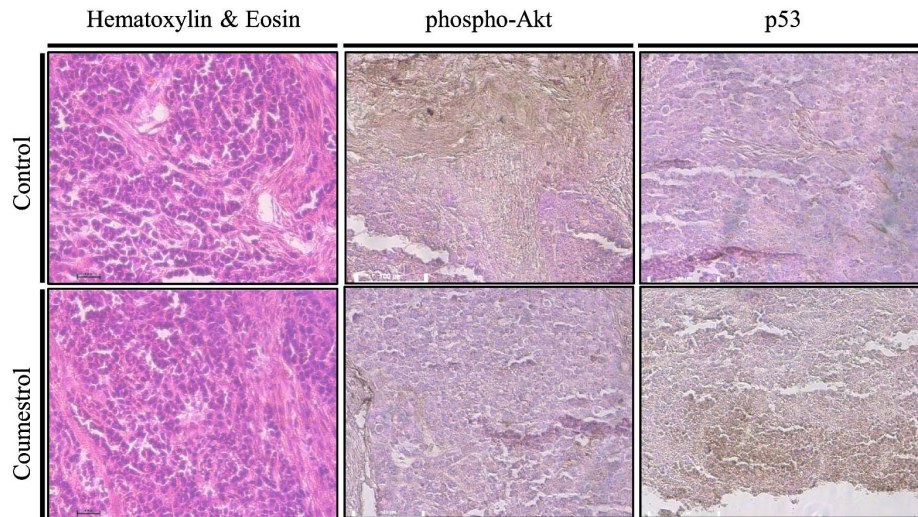


Figure 24. Coumestrol-induced antitumor effects are mediated by the modulation of the Akt cellular signaling pathway and upregulation of tumor suppressor p53 in the FaDu xenograft animal model. The control and coumestrol-treated mice sacrificed at the indicated intervals and tumor tissues were subjected to hematoxylin and eosin staining. Tumor tissues were dissected from xenograft animals, perfused, and fixed in saline and 4% paraformaldehyde, respectively. The dissected tumor tissues were post-fixed in 4% paraformaldehyde and embedded in paraffin for sectioning. Immunohistochemical staining of phospho-Akt and p53 was conducted and sections were counterstained using hematoxylin.

IV. Discussion

HNSCC, a malignant tumor that forms on the mucosal surfaces of the upper orogastrointestinal tract, including the oral cavity, pharynx, larynx, and paranasal sinuses, has previously been treated with either surgery alone or in combination with radiotherapy and chemotherapy, based on according to the tumor stage and location (Martino et al., 2008; Lydiatt et al., 2017). However, these clinical treatments for patients with HNSCC frequently resulted in a lower quality of life, owing side effects such as masticatory dysfunction and psychological problems caused by the alteration of the patient's orofacial appearance (Martino et al., 2008). Therefore, the development of chemotherapeutic reagents with fewer side effects and excellent antitumor activity needed to achieve cancer cell-specific death and reduce side effects. Furthermore, some recent studies, which have been associated with the development of chemotherapeutic reagents, have focused on the anticancer effects of natural compounds isolated from either herbal plants used in folk medicine or biologically-proven natural materials.

Phytoestrogens, which have a similar chemical structure to 17β -estradiol, are natural bioactive materials that are present in various edible herbal plants and fruits (Soni et al., 2014; Sirokin et al., 2014). Therefore, phytoestrogens can mediate the various physiological and pathological responses that are associated with reproduction, bone remodeling, cardiovascular function, immune system activity, and many other metabolic diseases, through interaction with the estrogen receptor (Sirotkin and Harrath, 2014). Moreover, recent studies have revealed that phytoestrogens prevent cancer and have been used as chemotherapeutic reagents in various cancers, including cancers of the liver, lung, colon, breast, prostate, and mouth (Heald et al., 2007). In addition, it was recently reported that biochanin-A, a phytoestrogen derived from *Trifolium pratense* (*T. pratense*), also known as red clover, induced the apoptosis of FaDu cells through both the death receptor-dependent (extrinsic)

and mitochondrial-dependent (intrinsic) pathways of apoptosis (Cho et al., 2017). In the present study, coumestrol, a phytoestrogen isolated from herbal plants, induced FaDu cell death through both the death receptor-mediated (extrinsic) and mitochondrial-dependent (intrinsic) apoptosis pathways and suppressed colony formation, wounding migration, and invasion *in vitro* and *in vivo*. For development as chemotherapeutic reagents, candidat materials must have biological safety and cause fewer side effects on normal tissues. Therefore, to verify the biological safety of coumestrol, the cytotoxicity of coumestrol was first assessed on the normal cells, as shown in Figure 2; treatment with 10 ~ 50 μ M coumestrol did not increase toxicity or survival in L929, which were used as normal cells. These data indicated that coumestrol has a high degree of biological safety in normal tissues and exerts fewer side effects in the defined treatment conditions. However, the cytotoxicity of FaDu cells was significantly increased in the does range of 20 ~ 50 μ M coumestrol, as shown in Figure 3. Collectively, these data suggested that coumestrol may act as a promising chemotherapeutic material with fewer side effects and specific toxicity to cancer cells and HNSCC. However, to verify the biological safety and the greater specificity of the toxicity to cancer cells, we conducted a, cell survival assay using a cell live & dead assay kit, composed of green calcein AM to stain the live cells with green fluorescence and ethidium homodimer-1 to stain the dead cells with red fluorescence (shown in Figures 4 and 5 in L929 [normal control cells] and in FaDu cells [cancer cells], respectively). As shown in Figure 4, 25 ~ 50 μ M coumestrol did not increase intensity of red fluorescence in L929, whereas, coumestrol not only decreased the total number of cells, but also increased the number of dead cells stained with red fluorescence when FaDu cells were concerned. The data have consistently suggested that as coumestrol has few side effects and may induce cancer cell-specific death, it may be a potential candidate chemotherapeutic material for the patients with HNSCC.

In general, cell death, including apoptosis and necrosis, is accompanied by morphological alterations, such as cell shrinkage including apoptotic body

formation (Bortner et al., 2007), nuclear condensation (Kass et al., 1996), and chromosomal DNA fragmentation (Higuchi, 2003). Therefore, to investigate the morphological alterations of FaDu cells in the presence or absence of coumestrol, H&E staining was performed (Figure 6). Many cells exhibited cytoplasmic shrinkage; moreover, the number of FaDu cells exhibiting nuclear shrinkage was significantly increased by treatment with coumestrol. Furthermore, the results of DAPI nuclear staining showed that the number of FaDu cells with condensed nuclei was increased in a dose-dependent manner by treatment with coumestrol (Figure 7). Moreover, chromosomal DNA fragmentation was significantly higher in FaDu cells than in the coumestrol-treated cells (Figure 8). In the present study, coumestrol induced morphological alteration in apoptotic bodies, chromatin condensation, and DNA fragmentation, which are typical characteristics of apoptosis (Bortner et al., 2007; Kass et al., 1996; Higuchi, 2003), in FaDu cells. Collectively, these data indicated that coumestrol-induced FaDu cell death was closely mediated by apoptotic cellular processes. Hence, to elucidate whether coumestrol induced the apoptosis in FaDu cells, FACS analysis of annexin-V and PI-stained was performed (Figure 9). Both cell of apoptotic cells populations (the early and late stages of apoptosis) were gradually increased in FaDu cells treated with coumestrol. These data strongly indicated that coumestrol induced the apoptosis of FaDu cells.

However, the targeted regulation of cellular mechanisms for the acceleration of cell death is a highly effective strategy for cancer therapy. Apoptosis is a particularly pivotal process that is associated with the elimination of unwanted cells during development to maintain homeostasis in long-lived mammals (Wang and Youle, 2009). Therefore, many recent studies have associated with the development of chemotherapeutic reagents have focused on the induction of cancer cell-specific apoptosis through the modulation of apoptotic signaling pathways (Jia et al., 2012). Apoptosis is generally classified into death receptor-mediated (extrinsic) and mitochondrial dependent

(intrinsic); apoptosis pathways (Khosravi-Far and Esposti, 2004). Notably, apoptosis is highly regulated by the activation (cleavage) of caspases (cysteine aspartyl-specific proteases) to induce cell death (Gray et al., 2010).

The death receptor-mediated (extrinsic) apoptosis pathway is triggered by the recruitment of adaptor proteins: such as Fas-associated death domain (FADD) and tumor necrosis factor (TNF) receptor-associated death domain (TRADD), and through the binding of death ligands: such as FasL, TNF-related apoptosis-inducing ligand (TRAIL), and TNF to TNF family death receptors (Zaman et al., 2014; Goldar et al., 2015; Liu et al., 2017). Subsequently, adaptor proteins induce the activation of caspase-8, through the cleavage of pro-caspase-8. Finally, activated caspase-8 induces the activation of executioner caspase-3, which leads to cell death (Goldar et al., 2015). Therefore, to investigate the coumestrol-induced apoptotic pathway, western blotting was performed (Figures 10-12).

As shown in Figure 10, coumestrol increased the expression of FasL and the activation of caspase-8 in FaDu cells. Furthermore, the activation of caspase-3 and its downstream pro-apoptotic substrate, PARP, was higher in FaDu cells than in the coumestrol-treated cells. These results consistently indicated that coumestrol-induced apoptosis was coordinated by the death receptor-mediated (extrinsic) apoptosis pathway, through an upregulation of the expression of death ligand FasL in FaDu cells. Generally, the mitochondrial-dependent (intrinsic) apoptosis pathway is initiated by the cleavage of Bid to tBid in response to apoptotic stress, such as damaged DNA, upregulated oncogenes, growth factor deprivation, increased Ca^{2+} levels, DNA-damaging molecules, oxidants, and microtubule-targeting drugs (Hassan et al., 2014). In addition, the activation of caspase-8, which is involved in the death receptor-mediated extrinsic apoptosis pathway, can initiate the mitochondrial-dependent intrinsic apoptosis pathway through the cleavage of Bid to tBid (Green et al., 2015). Subsequently, the oligomerization of activated Bax and Bak led to the release of intermembrane cytochrome c, through the induction of mitochondrial outer membrane permeabilization (Suhaili et al.,

2017). However, although the oligomerization of activated Bax and Bak is suppressed by anti-apoptotic factors such as Bcl-2 and Bcl-xL, the anti-apoptotic activity of Bcl-2 and Bcl-xL are regulated by pro-apoptotic factors, such as Bik, Bim, and Bad (Czabotar et al., 2009; Gogada et al., 2013). As shown in Figure 11, the activation of caspase-8 induced a decrease in Bid, through the cleavage of Bid to tBid, in FaDu cells treated with coumestrol. In addition, coumestrol induced a decrease in anti-apoptotic activities through the downregulation of the expression of anti-apoptotic factors, such as Bcl-2 and Bcl-xL in FaDu cells. Moreover, coumestrol increased the expression of mitochondrial-dependent pro-apoptotic factors, such as Bik, Bim, and Bad. Subsequently, alterations in the levels of these anti- and pro-apoptotic factors associated with the mitochondria-dependent apoptosis pathway induced the cascade activation of caspase-9, caspase-3, and PARP in FaDu cells treated with coumestrol as shown in Figure 12. Collectively, these data indicated that coumestrol-induced apoptosis was mediated by the mitochondrial-dependent (intrinsic) apoptosis pathway through the activation of caspase-8, which was triggered by the upregulation of FasL expression in FaDu cells. In support of this study, coumestrol was been found to induce mitochondrial-dependent apoptosis pathways through the downregulation of Bcl-2 expression and upregulation of Bax expression in human placental choriocarcinoma cells and, human breast cancer MCF-7 cells (Lim et al., 2017; Zafar et al., 2017). Collectively, these data indicate that coumestrol-induced apoptosis was mediated by both death receptor mediated (extrinsic) apoptosis triggered by upregulation of FasL, and mitochondrial dependent (intrinsic) apoptosis through the cleavage of Bid to tBid by cleaved caspase-8 in FaDu cells. Furthermore, coumestrol induced the activation of caspase-3 in a dose-dependent manner, which it was significantly counteracted by pan-caspase inhibitor Z-VAD-FMK (Figures 13-15). These results suggested that coumestrol-induced apoptosis in FaDu cells was mediated by the activation of caspase-3 and occurred through both the death receptor-mediated (extrinsic) and mitochondrial-dependent (intrinsic) apoptotic

pathways.

Migration and invasion of cancer cells to other tissues through the bloodstream and lymphatic system are generally observed in the terminal stage of cancer (Cho et al., 2017; Stec et al., 2011). Therefore, the inhibition of cancer cell growth and metastasis are crucial aims of clinical cancer treatment (Hsieh et al., 2017). In the present study, coumestrol significantly decelerated colony formation, wounding migration, and invasion in FaDu cells (Figures 16-18). Furthermore, MMPs, including MMP-2 and MMP-9, were closely associated with the invasion and metastasis of cancer cells and neoangiogenesis in cancer tissues (Marshall et al., 2000). Hence, the inhibition of MMP activation was a representative pharmacological target for cancer therapy (Marshall et al., 2000). As shown in Figure 19, the expression and activation of MMPs including MMP-2 and MMP-9, were significantly downregulated and suppressed by coumestrol in FaDu cells. These data suggested that coumestrol may have not only apoptotic effects, but also the suppress of metastasis in HNSCC. In addition, the phosphorylation of Akt and mTOR in FaDu cells was decreased after coumestrol treatment. Generally, the phosphorylation of Akt is triggered by the activation of PI3K, a phospholipid kinase, though interaction with receptor tyrosine kinases. After activation, PI3K converts its substrate phosphatidylinositol 4, 5-biphosphate (PIP₂) to phosphatidylinositol 3, 4, 5-triphosphate (PIP₃). PIP₃ then induces the phosphorylation of Akt, which is a serine-threonine kinase with an essential role as a cellular signaling molecule in cell survival, migration, cell cycle progression, and metabolism during development and carcinogenesis (Zhang et al., 2011). Notably, the activation of Akt signaling regulates the suppression of apoptosis in cancer cells, through either the reduction of pro-apoptotic factors Bad and Bax or the elevation of anti-apoptotic factors Bcl-2 and Bcl-xL. Therefore, the abnormal activation of Akt signaling pathologically accelerates tumorigenesis in human cancers (Crowell et al., 2007), which indicates that the targeted inhibition of Akt may suppress carcinogenesis and induce apoptosis. However, the activation of PI3K/Akt signaling is negatively

regulated by phosphatase and tensin homolog (PTEN) through the conversion of PIP3 to PIP2 (Okumura et al., 2012). In the present study, coumestrol dose-dependently suppressed the phosphorylation of Akt and its downstream target molecule mTOR in FaDu cells. Furthermore, many recent studies have reported p53 mutations in over 50% of all human cancers and highlighted the crucial role of p53 as a tumor suppressor in preventing cancer (Mello et al., 2017). In mammalian cells, p53 is a nuclear transcriptional factor that regulates apoptosis, cell cycle arrest, and senescence in response to cell stress. Furthermore, p53 increases mitochondrial outer membrane permeabilization and is associated with the mitochondrial-dependent apoptosis pathway through the upregulation of the expression of pro-apoptotic factors, such as Bax, Bad, and Bak (Tait et al., 2010). However, PTEN is inactivated by the phosphorylation of Akt, leading to the suppression of p53 expression. Conversely, PTEN activation increases the expression of p53 through the inactivation of Akt signaling (Yao et al., 2013). In the present study, the expression of p53 was dose-dependently increased in FaDu cells treated with coumestrol, (Figure 20). This indicated that the coumestrol-induced antitumor effects, including the induction of apoptosis, the attenuation of colony formation, and the suppression of wounding migration and invasion, were mediated by the alteration of the PI3K/Akt-mTOR axis and the upregulation of tumor suppressor p53 in FaDu cells.

However, cell division is regulated by the activation of cyclins, which interact with the cyclin-dependent kinases (CDKs) to induce cell-cycle progression (Coqueret, 2003). Therefore, the regulation of the cell cycle has become a chemotherapeutic targeting strategy to combat associated with the proliferation, migration, and invasion of cancer cells. In particular, the upregulation of the cell cycle inhibitors such as the p21 and p27 *Cip/Kip* proteins induce the cell arrest to attenuate the proliferation, migration, and invasion of cancer cells (Roy et al., 2007). In the present study, the expression of p21 and p27 were significantly increased in FaDu cells treated with coumestrol (Figure 21). These data indicated that coumestrol-induced

anticancer effects such as the suppression of colony formation through the attenuation of proliferation and the deceleration of wounding migration and invasion, were closely associated with cell-cycle arrest through the modulation of cell-cycle inhibitors, such as the p21 and p27 *Cip/Kip* proteins in FaDu cells.

Another cellular signaling molecule associated with carcinogenesis, MAPK, is closely involved with tumor cell proliferation, differentiation, apoptosis, angiogenesis, invasion, and metastasis (Peng et al., 2018) through the expression of MMPs including MMP-2 and MMP-9. As shown in Figure 22, the phosphorylation of ERK1/2 and p38 was significantly and dose-dependently suppressed in FaDu cells treated with coumestrol. Recent studies have reported that the MAPK signaling pathway may directly or indirectly suppress the activation of caspase-3 and caspase-9 through the inhibition of the release of cytochrome *c* from mitochondria (Peng et al., 2018; Huang et al., 2017; Lv et al., 2017; Chen et al., 2016). Recently, Lim et al. reported that coumestrol inhibited proliferation and migration of prostate cancer cells through the regulation of AKT, and ERK1/2-MAPK cellular signaling cascades, which was similar to the results of present study. Therefore, as the MAPK signaling pathway is frequently activated in cancer cells, the inactivation of this signaling pathway may contribute to antitumor effects.

To evaluate the *in vivo* antitumor effects of coumestrol, animals were xenografted with FaDu cells and orally administrated coumestrol for 21 days; the observed changes are in Figure 23. The oral administration of coumestrol effectively suppressed the tumor growth compared with the control animal. Furthermore, the histology results (Figure 24) showed that the expression of tumor suppressor p53 was significantly upregulated in the tumor tissues dissected from xenograft animals administered coumestrol compared with those in the control group. Moreover, the phosphorylation of Akt was significantly suppressed in the tumor tissues in the animals administered coumestrol. Hence, these data indicated that both the suppression of PI3K/Akt and the upregulation of p53 were crucial factors associated with the

coumestrol-induced antitumor effects in HNSCC.

In conclusion, coumestrol effectively induced cell death through both the death receptor-mediated (extrinsic) and mitochondrial-dependent (intrinsic) apoptosis pathways in FaDu cells. Furthermore, coumestrol-induced apoptosis was involved in the upregulation of p53 expression, through the inactivation of Akt-mTOR axis and the MAPK cellular signaling pathways in FaDu cells. These findings suggest that coumestrol may be a promising candidate chemotherapeutic agent for the treatment of HNSCC.

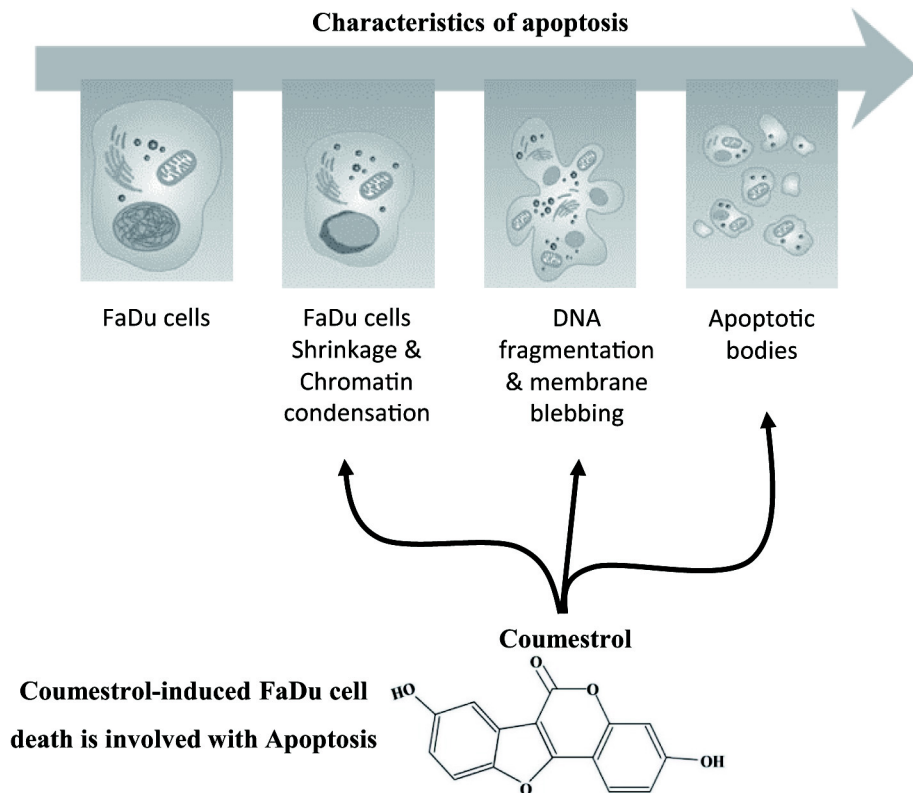
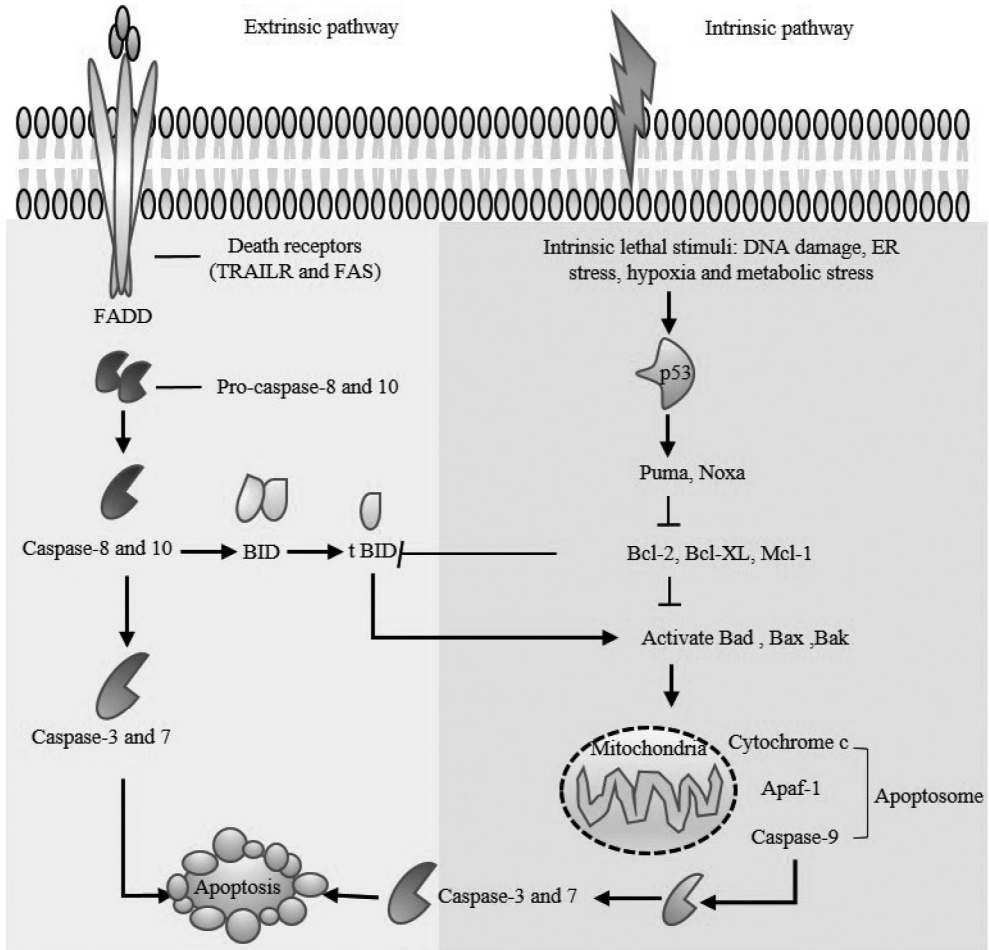


Figure 25. Schematic diagram of the coumestrol-induced apoptotic phenomenon.



Coumestrol induces FaDu cell death through both Death receptor mediated extrinsic and mitochondrial dependent intrinsic apoptosis pathways

Figure 26. Schematic diagram of coumestrol-induced apoptosis pathways.

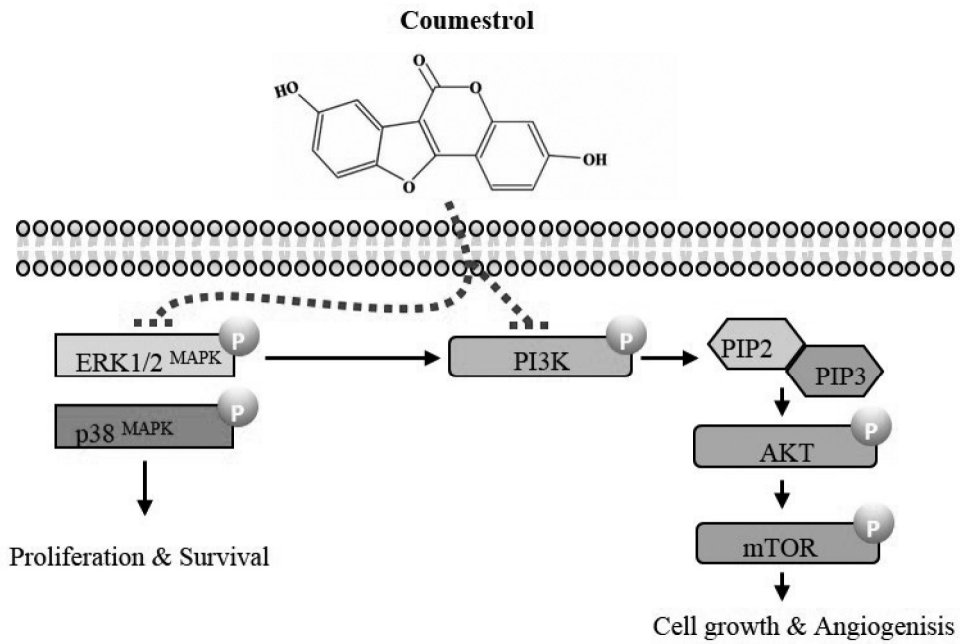


Figure 27. Schematic diagram of cellular signaling pathways associated with the coumestrol-induced inhibition of migration and invasion in FaDu cells.

V. References

1. Bacciottini, L., Falchetti, A., Pampaloni, B., Bartolini, E., Carossino, A.M. and Brandi, M.L., 2007. Phytoestrogens: food or drug? *Clin Cases Miner Bone Metab* 4, 123-30.
2. Bortner C.D., and Cidlowski J.A., 2007. Cell shrinkage and monovalent cation fluxes: Role in apoptosis. *Arch Biochem Biophys* 462, 176-188.
3. Boscolo-Rizzo, P., Zorzi, M., Del Mistro, A., Da Mosto, M.C., Tirelli, G., Buzzoni, C., Rugge, M., Polesel, J. and Guzzinati, S., 2018. The evolution of the epidemiological landscape of head and neck cancer in Italy: Is there evidence for an increase in the incidence of potentially HPV-related carcinomas? *PLoS One* 13, e0192621
4. Ceccarelli, M., Rullo, E.V., Facciola, A., Madeddu, G., Cacopardo, B., Taibi, R., D'Aleo, F., Pinzone, M.R., Picerno, I., di Rosa, M., Visalli, G., Condorelli, F., Nunnari, G. and Pellicano, G.F., 2018. Head and neck squamous cell carcinoma and its correlation with human papillomavirus in people living with HIV: a systematic review. *Oncotarget* 9, 17171-17180.
5. Chen, H., Jin, Z.L., and Xu, H., 2016. MEK/ERK signaling pathway in apoptosis of SW620 cell line and inhibition effect of resveratrol. *Asian Pac J Trop Med* 9, 49-53.
6. Chen, L. and Hu, G.F., 2010. Angiogenin-mediated ribosomal RNA transcription as a molecular target for treatment of head and neck squamous cell carcinoma. *Oral Oncol* 46, 648-53.
7. Chien, Y.C., Chen, J.Y., Liu, M.Y., Yang, H.I., Hsu, M.M., Chen, C.J. and Yang, C.S., 2001. Serologic markers of Epstein-Barr virus infection and nasopharyngeal carcinoma in Taiwanese men. *N Engl J Med* 345, 1877-82.
8. Cho I.A., You S.J., Kang K.R., Kim S.G., Oh J.S., You J.S., Lee G.J., Seo Y.S., Kim D.K., Kim C.S., Lee S.Y., and Kim J.S., 2017. Biochanin-A induces apoptosis and suppresses migration in FaDu human pharynx squamous carcinoma cells. *Oncol Rep* 38, 2985-2992.
9. Crowell, J.A., Steele, V.E. and Fay, J.R., 2007. Targeting the AKT protein kinase for cancer chemoprevention. *Molecular Cancer Therapeutics* 6, 2139-2148.
10. Coqueret, O., 2003. New roles for p21 and p27 cell-cycle inhibitors: a

- function for each cell compartment? Trends Cell Biol 13, 65–70.
11. Czabotar P.E., Colman P.M., and Huang D.C., 2009. Bax activation by Bim? Cell Death Differ 16, 1187–1191.
 12. Dattatreya, S., 2013. Metastatic colorectal cancer—prolonging overall survival with targeted therapies. South Asian J Cancer 2, 179–85.
 13. Desai, A.G., Qazi, G.N., Ganju, R.K., El-Tamer, M., Singh, J., Saxena, A.K., Bedi, Y.S., Taneja, S.C. and Bhat, H.K., 2008. Medicinal plants and cancer chemoprevention. Curr Drug Metab 9, 581–91.
 14. Galbiatti, A.L., Padovani-Junior, J.A., Maniglia, J.V., Rodrigues, C.D., Pavarino, E.C. and Goloni-Bertollo, E.M., 2013. Head and neck cancer: causes, prevention and treatment. Braz J Otorhinolaryngol 79, 239–47.
 15. Gaya, P., Medina, M., Sanchez-Jimenez, A. and Landete, J.M., 2016. Phytoestrogen Metabolism by Adult Human Gut Microbiota. Molecules 21.
 16. Gray, D.C., Mahrus, S. and Wells, J.A., 2010. Activation of Specific Apoptotic Caspases with an Engineered Small Molecule-Activated Protease. Cell 142, 637–646.
 17. Gogada R., Yadav N., Liu J., Tang S., Zhang D., Schneider A., Seshadri A., Sun L., Aldaz C.M., Tang D.G., and Chandra D., 2013. Bim, a proapoptotic protein, up-regulated via transcription factor E2F1-dependent mechanism, functions as a prosurvival molecule in cancer. J Biol Chem 288, 368–381.
 18. Goldar S., Khaniani M.S., Derakhshan S.M., and Baradaran B., 2015. Molecular mechanisms of apoptosis and roles in cancer development and treatment. Asian Pac J Cancer Prev 16, 2129–2144.
 19. Green D.R., and Llambi F., 2015. Cell Death Signaling. Cold Spring Harb Perspect Biol 7
 20. Guenin, S., Mouallif, M., Hubert, P., Jacobs, N., Krusy, N., Duray, A., Ennaji, M.M., Saussez, S. and Delvenne, P., 2014. Interleukin-32 expression is associated with a poorer prognosis in head and neck squamous cell carcinoma. Mol Carcinog 53, 667–73.
 21. Gupta, G.P. and Massague, J., 2006. Cancer metastasis: building a framework. Cell 127, 679–95.
 22. Hashibe, M., Brennan, P., Chuang, S.C., Boccia, S., Castellsague, X., Chen, C., Curado, M.P., Dal Maso, L., Daudt, A.W., Fabianova, E., Fernandez, L., Wunsch-Filho, V., Franceschi, S., Hayes, R.B., Herrero, R., Kelsey, K.,

- Koifman, S., La Vecchia, C., Lazarus, P., Levi, F., Lence, J.J., Mates, D., Matos, E., Menezes, A., McClean, M.D., Muscat, J., Eluf-Neto, J., Olshan, A.F., Purdue, M., Rudnai, P., Schwartz, S.M., Smith, E., Sturgis, E.M., Szeszenia-Dabrowska, N., Talamini, R., Wei, Q., Winn, D.M., Shangina, O., Pilarska, A., Zhang, Z.F., Ferro, G., Berthiller, J. and Boffetta, P., 2009. Interaction between tobacco and alcohol use and the risk of head and neck cancer: pooled analysis in the International Head and Neck Cancer Epidemiology Consortium. *Cancer Epidemiol Biomarkers Prev* 18, 541-50.
23. Hassan M., Watari H., AbuAlmaaty A., Ohba Y., and Sakuragi N., 2014. Apoptosis and molecular targeting therapy in cancer. *Biomed Res Int* 2014, 150845.
24. Higuchi Y, 2003. Chromosomal DNA fragmentation in apoptosis and necrosis induced by oxidative stress. *Biochem Pharmacol* 66, 1527-1535.
25. Hsieh M.J., Chen J.C., Yang W.E., Chien S.Y., Chen M.K., Lo Y.S., Hsi Y.T., Chuang Y.C., Lin C.C., and Yang S.F., 2017. Dehydroandrographolide inhibits oral cancer cell migration and invasion through NF-kappaB-, AP-1-, and SP-1-modulated matrix metalloproteinase-2 inhibition. *Biochem Pharmacol* 130, 10-20.
26. Huang, R.H., Quan, Y.J., Chen, J.H., Wang, T.F., Xu, M., Ye, M., Yuan, H., Zhang, C.J., Liu, X.J., and Min, Z.J., 2017. Osteopontin Promotes Cell Migration and Invasion, and Inhibits Apoptosis and Autophagy in Colorectal Cancer by activating the p38 MAPK Signaling Pathway. *Cell Physiol Biochem* 41, 1851-1864.
27. Heald, C.L., Ritchie, M.R., Bolton-Smith, C., Morton, M.S. and Alexander, F.E., 2007. Phyto-oestrogens and risk of prostate cancer in Scottish men. *Br J Nutr* 98, 388-96.
28. Jakobi, A., Bandurska-Luque, A., Stutzer, K., Haase, R., Lock, S., Wack, L.J., Monnich, D., Thorwarth, D., Perez, D., Luhr, A., Zips, D., Krause, M., Baumann, M., Perrin, R. and Richter, C., 2015. Identification of Patient Benefit From Proton Therapy for Advanced Head and Neck Cancer
29. Jantaratnotai, N., Utaisinchaoen, P., Sanvarinda, P., Thampithak, A. and Sanvarinda, Y., 2013. Phytoestrogens mediated anti-inflammatory effect through suppression of IRF-1 and pSTAT1 expressions in lipopolysaccharide-activated microglia. *Int Immunopharmacol* 17, 483-8.
30. Jemal, A., Siegel, R., Ward, E., Murray, T., Xu, J. and Thun, M.J., 2007.

- Cancer statistics, 2007. *CA Cancer J Clin* 57, 43-66.
31. Jia, L.-T., Chen, S.-Y. and Yang, A.-G., 2012. Cancer gene therapy targeting cellular apoptosis machinery. *Cancer Treatment Reviews* 38, 868-876.
 32. Kass G.E., Eriksson J.E., Weis M., Orrenius S., and Chow S.C., 1996. Chromatin condensation during apoptosis requires ATP. *Biochem J* 318 (Pt 3), 749-752.
 33. Khorasani Esmaeili, A., Mat Taha, R., Mohajer, S. and Banisalam, B., 2015. Antioxidant Activity and Total Phenolic and Flavonoid Content of Various Solvent Extracts from In Vivo and In Vitro Grown *Trifolium pratense* L. (Red Clover). *Biomed Res Int* 2015, 643285.
 34. Kinghorn, A.D., Pan, L., Fletcher, J.N. and Chai, H., 2011. The Relevance of Higher Plants in Lead Compound Discovery Programs(). *Journal of natural products* 74, 1539-1555.
 35. Li, J.W. and Vederas, J.C., 2011. [Drug discovery and natural products: end of era or an endless frontier?]. *Biomed Khim* 57, 148-60.
 36. Lim W., Yang C., Jeong M., Bazer F.W., and Song G., 2017. Coumestrol induces mitochondrial dysfunction by stimulating ROS production and calcium ion influx into mitochondria in human placental choriocarcinoma cells. *Mol Hum Reprod* 23, 786-802.
 37. Lim, W., Jeong, M., Bazer, F.W., and Song, G., 2017. Coumestrol inhibits proliferation and migration of prostate cancer cells by regulating AKT, ERK1/2, and JNK MAPK cell signaling cascades. *J Cell Physiol* 232, 862-871.
 38. Liu H., Su D., Zhang J., Ge S., Li Y., Wang F., Gravel M., Roulston A., Song Q., Xu W., Liang J.G., Shore G., Wang X., and Liang P., 2017. Improvement of Pharmacokinetic Profile of TRAIL via Trimer-Tag Enhances its Antitumor Activity in vivo. *Sci Rep* 7, 8953.
 39. Lu, Y.H., Gao, X.Q., Wu, M., Zhang-Negrerie, D. and Gao, Q., 2011. Strategies on the development of small molecule anticancer drugs for targeted therapy. *Mini Rev Med Chem* 11, 611-24.
 40. Luce, D., Gerin, M., Leclerc, A., Morcet, J.F., Brugere, J. and Goldberg, M., 1993. Sinonasal cancer and occupational exposure to formaldehyde and other substances. *Int J Cancer* 53, 224-31.
 41. Luo, X., Qiu, Y., Jiang, Y., Chen, F., Jiang, L., Zhou, Y., Dan, H., Zeng, X.,

- Lei, Y.L. and Chen, Q., 2018. Long non-coding RNA implicated in the invasion and metastasis of head and neck cancer: possible function and mechanisms. *Mol Cancer* 17, 14.
42. Lv, D., Wu, H., Xing, R., Shu, F., Lei, B., Lei, C., Zhou, X., Wan, B., Yang, Y., Zhong, L., Mao, X., and Zou, Y., 2017. HnRNP-L mediates bladder cancer progression by inhibiting apoptotic signaling and enhancing MAPK signaling pathways. *Oncotarget* 8, 13586-13599.
43. Lydiatt W.M., Patel S.G., O'Sullivan B., Brandwein M.S., Ridge J.A., Migliacci J.C., Loomis A.M., and Shah J.P., 2017. Head and Neck cancers-major changes in the American Joint Committee on cancer eighth edition cancer staging manual. *CA Cancer J Clin* 67, 122-137.
44. Marshall J.L., Baidas S., Bhargava P., and Rizvi N., 2000. Matrix metalloproteinase inhibitors in cancer: an update. *IDrugs* 3, 518-524.
45. Martino R. and Ringash J., 2008. Evaluation of quality of life and organ function in head and neck squamous cell carcinoma. *Hematol Oncol Clin North Am* 22, 1239-1256.
46. Mello S.S., and Attardi L.D., 2017. Deciphering p53 signaling in tumor suppression. *Curr Opin Cell Biol* 51, 65-72.
47. Okumura N., Yoshida H., Kitagishi Y., Murakami M., Nishimura Y., and Matsuda S., 2012. PI3K/AKT/PTEN Signaling as a Molecular Target in Leukemia Angiogenesis. *Adv Hematol* 2012, 843085.
48. Peng, Q., Deng, Z., Pan, H., Gu, L., Liu, O., and Tang, Z., 2018. Mitogen-activated protein kinase signaling pathway in oral cancer. *Oncol Lett* 15, 1379-1388.
49. Pandey, K.B. and Rizvi, S.I., 2009. Plant polyphenols as dietary antioxidants in human health and disease. *Oxidative Medicine and Cellular Longevity* 2, 270-278.
50. Pinna, R., Campus, G., Cumbo, E., Mura, I. and Milia, E., 2015. Xerostomia induced by radiotherapy: an overview of the physiopathology, clinical evidence, and management of the oral damage. *Ther Clin Risk Manag* 11, 171-88.
51. Radhakrishnan, A., Nanjappa, V., Raja, R., Sathe, G., Puttamalles, V.N., Jain, A.P., Pinto, S.M., Balaji, S.A., Chavan, S., Sahasrabudhe, N.A., Mathur, P.P., Kumar, M.M., Prasad, T.S., Santosh, V., Sukumar, G., Califano, J.A., Rangarajan, A., Sidransky, D., Pandey, A., Gowda, H. and

- Chatterjee, A., 2016. A dual specificity kinase, DYRK1A, as a potential therapeutic target for head and neck squamous cell carcinoma. *Sci Rep* 6, 36132.
52. Reger, M.K., Zollinger, T.W., Liu, Z., Jones, J.F. and Zhang, J., 2018. Dietary intake of isoflavones and coumestrol and the risk of prostate cancer in the Prostate, Lung, Colorectal and Ovarian Cancer Screening Trial. *Int J Cancer* 142, 719–728.
53. Roy, S., Kaur, M., Agarwal, C., Tecklenburg, M., Sclafani, R.A. and Agarwal, R., 2007. P21 and p27 induction by silibinin is essential for its cell cycle arrest effect in prostate carcinoma cells. *Molecular Cancer Therapeutics* 6, 2696–2707.
54. Shrotriya, S., Agarwal, R. and Sclafani, R.A., 2015. A perspective on chemoprevention by resveratrol in head and neck squamous cell carcinoma. *Adv Exp Med Biol* 815, 333–48.
55. Sirotkin A.V., and Harrath A.H., 2014. Phytoestrogens and their effects. *Eur J Pharmacol* 741, 230–236.
56. Soni M., Rahardjo T.B., Soekardi R., Sulistyowati Y., Lestariningsih, Yesufu-Udechuku A., Irsan A., and Hogervorst E., 2014. Phytoestrogens and cognitive function: a review. *Maturitas* 77, 209–220.
57. Stec R., Bodnar L., Smoter M., Maczewski M., and Szczylik C., 2011. Metastatic colorectal cancer in the elderly: An overview of the systemic treatment modalities (Review). *Oncol Lett* 2, 3–11.
58. Suhaili S.H., Karimian H., Stellato M., Lee T.H., and Aguilar M.I., 2017. Mitochondrial outer membrane permeabilization: a focus on the role of mitochondrial membrane structural organization. *Biophys Rev* 9, 443–457.
59. Tait, S.W., and Green, D.R., 2010. Mitochondria and cell death: outer membrane permeabilization and beyond. *Nat Rev Mol Cell Biol* 11, 621–632.
60. Tang, G.Y., Meng, X., Li, Y., Zhao, C.N., Liu, Q. and Li, H.B., 2017. Effects of Vegetables on Cardiovascular Diseases and Related Mechanisms. *Nutrients* 9.
61. Taylor, W.F. and Jabbarzadeh, E., 2017. The use of natural products to target cancer stem cells. *American Journal of Cancer Research* 7, 1588–1605.
62. Wang, C. and Youle, R.J., 2009. The Role of Mitochondria in Apoptosis().

- Annual review of genetics 43, 95-118.
63. Yao, C., Wei, J.J., Wang, Z.Y., Ding, H.M., Li, D., Yan, S.C., Yang, Y.J., and Gu, Z.P., 2013. Perifosine induces cell apoptosis in human osteosarcoma cells: new implication for osteosarcoma therapy? *Cell Biochem Biophys* 65, 217-227.
 64. Yu, M.C. and Yuan, J.M., 2002. Epidemiology of nasopharyngeal carcinoma. *Semin Cancer Biol* 12, 421-9.
 65. Zafar A., Singh S., and Naseem I., 2017. Cytotoxic activity of soy phytoestrogen coumestrol against human breast cancer MCF-7 cells: Insights into the molecular mechanism. *Food Chem Toxicol* 99, 149-161.
 66. Zafar, A., Singh, S., Satija, Y.K., Saluja, D. and Naseem, I., 2018. Deciphering the molecular mechanism underlying anticancer activity of coumestrol in triple-negative breast cancer cells. *Toxicol In Vitro* 46, 19-28.
 67. Zaman S., Wang R., and Gandhi V., 2014. Targeting the apoptosis pathway in hematologic malignancies. *Leuk Lymphoma* 55, 1980-1992.
 68. Zhang X., Tang N., Hadden T.J., and Rishi A.K., 2011. Akt, FoxO and regulation of apoptosis. *Biochim Biophys Acta* 1813, 1978-1986